ISSN 2277-2685
IJPSL/July. 2023/ Vol-13/Issue-3/1-42
Dr. MOHD YUNOOS *et. al* International Journal of Pharmacetical Sciences Letters

Phytochemical Analysis and Evaluation of Antioxidant and Antimicrobial Properties of Essential Oils and Seed Extracts of *Anethum graveolens* from Southern Morocco: In Vitro andIn Silico Approach for a Natural Alternative to Synthetic Preservatives

Dr. MOHD YUNOOS, Mrs. VENKATA KUMARI MUDIGONDA, Mr. M PRAVEEN PROFESSOR1 , Associate Professor2, Asst Prof3 M. PHARMACY-Pharmaceutical Analysis, 1 B.PHARMACY Nimra College of Pharmacy, Jupudi, Krishna District, Andhra Pradesh-521456

A. Article Info

Received: 03-03-2023 ***Revised: 20 -04-2023*** ***Accepted: 20-06-2023***

Abstract: The fragrant herb Anethum graveolens has a long history of medicinal usage, particularly as an antispasmodic and carminative. Essential oils and seed extracts collected in Errachidia, southern Morocco, will have their chemical compositions examined in this research. We will also test these oils and extracts for antibacterial and anti-oxidant capabilities. According to the GC-MS results, the primary components of the hydrodistillation-isolated EO were E-anethole (38.13%), es-tragole (29.32%), fenchone (17.21%), and α-pinene (7.37%). Using decoction and Soxhlet extraction techniques, the phenolic components were removed. Different extracts of A. graveolens had varying concentrations of polyphenols, flavonoids, and condensed tannins, according to the phenolic compound test. The decoction was subjected to HPLC/UV-ESI-MS tests, which revealed a wide range of molecular structures. Among these, the most significant ones were 12.35% umbelliferone, 11.23% 3-hydroxyflavone, 8.95% rosmanol, 8.36% bi-otin, 4.91% emmotin H, and 4.21% coumarin. The antioxidant activity, as measured by three methods (DPPH•, FRAP, and CAT), showed that the extracts and essential oils (EOs) could effectively fight harmful free radicals, regulate the production of reactive oxygen species, and reduce oxidative damage. Eos and extracts were tested in a liquid media for their antibacterial activity against five different strains of bacteria: E. cloacae, K. pneumoniae, E. coli, S. aureus, and S. epidermidis. Additionally, they were tested against four different types of candidiasis: C. albicans, C. dubliniensis, C. tropicalis, and C. parapsilosis, as well as Aspergillus niger. When compared to the aqueous, ethanolic, and decoction extracts, the findings demonstrated that the EOs were more efficient against the majority of the bacteria tested. Not only that, but the antifungal activity of the ethanolic extract was different from the other extracts. The study's essential oils' antimicrobial properties are mainly due to the synergistic interactions of E-anethole, estragole, and fenchone, which are its three main ingredients. The chosen bioactive chemicals interact and stabilize with several target proteins that have antioxidant and antibacterial effects, according to molecular docking and molecular dynamics simulation studies. With stronger binding energies to the investigated proteins, compounds such as 3-hydroxyflavone, emmotin H, trans-caftaric acid, me-thyl rosmarinate, 1-caffeoyl-beta-D-glucose, and kaempferol showed promise as antioxidant and antibacterial agents. Finally, our results highlight the importance of A. graveolens seeds as a potential source of bioactive substances with positive health effects that potentially replace synthetic preservatives on the market today.

Keywords: *Anethum graveolens*; GC/MS; HPLC/UV-ESI-MS; polyphenols; flavonoids; antioxidants; antimicrobials

1. Introduction

Particularly in underdeveloped nations, food poisoning is a major problem that affects people's health and the economy [1]. Antimicrobial resistance was a factor in 4.95 million deaths in 2023 and 1.27 million deaths in 2019, according to the World Health Organization (WHO). Extensive research is being carried out to produce novel antimicrobial agents and healthy food items in response to these concerning tendencies.
The induction of DNA damage and toxicity by synthetic preservatives like BHA and BHT has led to their restriction in usage for food degradation prevention [2,3]. Customers worry about the potential negative impact on human health from this vantage point. This reality has prompted businesses and individuals to seek for and use natural compounds that possess antioxidant and antibacterial characteristics. Essential oils and plant extracts used in medicine are examples of these all-natural compounds. Many people believe that these plants contain medicinally useful active secondary metabolites. Pathogens, herbivores, and competitors are the main targets of these chemicals in defensive processes [4]. Numerous sectors, including medicine, food production, personal care, and industrial raw materials, have benefited greatly from plant-based products. Really, they do double duty: first, they enhance the flavor of food, and second, they prevent spoilage by acting as an antioxidant and antibacterial, thereby postponing the food's degradation. Anethum graveolens, more often known as dill, is a prominent herb used in the pharmaceutical and agri-food industries [5]. As the only member of the Anethum genus, this perennial herb belongs to the Apiaceae family. Normally, it may grow to be 40 to 60 cm tall.
Countries in Eurasia and the Mediterranean cultivate dill, a noteworthy herb. The Egyptians and the Greeks have used its seeds and leaves as a spice and herb for seasoning food for five thousand years [6]. Traditional medicine often uses dill to soothe young children's gas and colic. Its seeds are also used in decoction or infusion form to treat gastrointestinal spasms, meteorism-related digestive problems, sleeplessness, hyposecretion of milk, and urinary tract infections [6,7]. Sauces, salads, soups, seafood, meats, fries, pickles, and pickles are just a few of the numerous culinary items that often use it as a natural taste enhancer. The aromatic volatile oil collected from the topsoil is used to improve the flavor of food and drink because of its pleasant aroma. Soaps, detergents, and cosmetics may all benefit from the aromatic properties of essential oils [8,9].

Scientific investigations have shown that Anethum graveolens has a wide range of biological potential, including anti-inflammatory, antidiabetic, antimicrobial, diuretic, insecticidal, hepatoprotective, anticancer, and antioxidant properties [10–16].
This species' fascinating traits have significantly increased its worldwide economic importance. There is ecological, socioeconomic, and therapeutic value to this plant in Morocco. Unfortunately, not much is known about the biological properties and chemical make-up of the essential oils and extracts produced by Anethum graveolens in Morocco. of particular, we looked at the chemical components of the Boulemane area's Anethum Graveolens seed extract and essential oil. Determining naturally occurring ring chemical compounds with antioxidant properties and evaluating their antioxidant and

conducted in vitro tests on the antimicrobial properties of essential oils and extracts from this species. However, the chemical makeup of Anethum graveolens seed extracts has only been the subject of a small amount of investigation. This research was carried out with the intention of adding to the existing body of knowledge on phytochemical analysis and chemical family characterisation in Anethum graveolens seeds collected from the Boulemane area. Furthermore, it comprises testing the

essential oils and extracts for antibacterial and antioxidant capabilities using in vitro and in silico methodologies to discover whether they have any antimicrobial or antioxidant potential.

2. Results & Discussion

2.1. Quality Control of Plant Material

The quality control findings of the examined plant material are displayed in Table 1. The seeds of *A. graveolens* had a moisture content of around 15.80%, which was within the typical range for seeds. The plant extract had a pH that was somewhat acidic, which aligned with its mineral content of 15.03%. This pH level meets the quality criteria set by AFNOR (NF ISO 5984).

Table 1. Analysis and quality control of *A. graveolens* seeds.

MC (%)	pH	Ash (%)	Organic Matter (%)
15.80	5.2	15.03	84.97

Medicinal plants, despite their health advantages, frequently become polluted by different agents or poisonous compounds during their cultivation and processing. Out of these, heavy metals are particularly worrisome since they can disrupt the proper operation of the central nervous system, liver, lungs, heart, kidneys, and brain. This disruption can result in hypertension, stomach aches, skin rashes, intestinal ulcers, and different types of cancer. In order to tackle this problem, we utilized atomic absorption spectrophotometry to analyze the concentration of six specific heavy metals: chromium (Cr), lead (Pb), cadmium (Cd), iron (Fe), antimony (Sb), and titanium (Ti).

According to the results shown in Table 2, Aneth seeds exhibit a high content of iron (Fe) at 0.5858 mg/L, followed by antimony (Sb) with a content of 0.0087 mg/L. Regarding the other detected heavy metals, it is noteworthy that they all fall within the allowable range set by FAO/WHO regulatory standards. Consequently, the studied plant is suitable for direct consumption, as an ingredient in food processing, or for repackaging if necessary.

Table 2. Heavy metal concentration (mg/L) and maximum limit FAO/WHO (2009).

Element	Heavy Metal Content (mg/L)	Maximum Limit
Chromium (Cr)	0.0008	2
Antimony (Sb)	0.0134	1
Lead (Pb)	0.0034	3
Cadmium (Cd)	<0.0001	0.3
Iron (Fe)	0.5858	20
Titanium (Ti)	0.0082	-

2.2. Physical-Chemical Properties and Extraction Yield of Essential Oils

The data reported in Table 3 indicate that the essential oils (EOs) obtained from the seeds of *A. graveolens* gathered in the Errachidia region during full bloom were characterized by an aromatic scent, a yellowish hue, and a yield of 2.73 ± 0.12%.

Notably, this result was, on the one hand, significant compared to those from other origins: in Egypt 1.88% [17], in India 1.5% [9], in Iran (0.04–1.86%) [18], and also within

the same country 1.92% [19]. On the other hand, it was lower than those reported elsewhere: in southern Morocco (3.5%) [20] and in China (6.7%) [21]. Based on the literature results and those obtained in this study, the variation in EO yield is attributed to various genetic, ecological, and environmental factors (plant age, climatic conditions, soil type, growth stage of the species, part used, harvest time, drying process, harvest period and environment, and cultural practices) as well as the extraction method used.

The plant under investigation yielded essential oils with a density of 0.9362 ± 0.0732 g/mL. Based on the AFNOR standard (2005), essential oils are advised to have a density ranging from 0.906 g/mL, which indicates lesser grade oils, to 0.990 g/mL, which is suggestive of oils of extremely high quality. The measurement indicates that the density of our essential oil is comfortably within the allowed range, indicating a quality that meets or exceeds the normal standards for essential oil density. This discovery suggests that the essential oil extracted from this plant possesses a praiseworthy quality that meets the standards set by the industry.

Table 3. Essential Oil Yield of *A. graveolens*.

Properties	Yield (%)	Color	Odor	Density (g/mL)
Results	2.73 ± 0.12	Yellowish	Aromatic	0.9362 ± 0.0032

2.3. Chemical Composition of EO

The chemical profile (Supplementary Figure S1) revealed the presence of 29 chemical compounds for the total chemical composition of this essential oil. These results are summarized in Table 4.

Table 4. Chemical Composition of *Anethum graveolens* Essential Oil.

N°	Compounds	KI*	RA%	Formula
1	α-Pinene	939	7.37	$C_{10}H_{16}$
2	Camphene	954	0.08	$C_{10}H_{16}$
3	Sabinene	975	0.13	$C_{10}H_{16}$
4	β-Pinene	979	0.35	$C_{10}H_{16}$
5	Myrcene	990	0.76	$C_{10}H_{16}$
6	α-Phellandrene	1002	0.17	$C_{10}H_{16}$
7	α-Terpinene	1017	0.02	$C_{10}H_{16}$
8	Limonene	1029	1.24	$C_{10}H_{16}$
9	β-Phellandrene	1029	0.37	$C_{10}H_{16}$
10	Z-β-Ocimene	1037	0.16	$C_{10}H_{16}$
11	1,8-Cineole	1031	0.11	$C_{10}H_{18}O$
12	γ-Terpinene	1059	0.66	$C_{10}H_{16}$
13	Terpinolene	1088	0.05	$C_{10}H_{16}$
14	**Fenchone**	**1086**	**17.21**	$C_{10}H_{16}O$
15	Linalool	1096	2.68	$C_{10}H_{18}O$
16	trans-Pinene hydrate	1122	0.03	$C_{10}H_{18}O$
17	Camphor	1146	0.35	$C_{10}H_{16}O$
18	Terpinen-4-ol	1177	0.13	$C_{10}H_{18}O$
19	**Estragole**	**1196**	**29.32**	$C_{10}H_{12}O$
20	Carvone	1243	0.01	$C_{10}H_{14}O$
21	Z-Anethole	1252	0.06	$C_{10}H_{12}O$
22	ϱ-Anis aldehyde	1250	0.05	$C_8H_8O_2$
23	**E-Anethole**	**1284**	**38.13**	$C_{10}H_{12}O$
24	α-Copaene	1376	0.02	$C_{15}H_{24}$

25	Z-Isoeugenol	1407	0.02	$C_{10}H_{12}O_2$
26	Methyleugenol	1403	0.34	$C_{11}H_{14}O_2$
27	Germacrene D	1481	0.09	$C_{15}H_{24}$
28	δ-Cadinene	1523	0.03	$C_{15}H_{24}$
29	E-Methylisoeugenol	1492	0.06	$C_{11}H_{14}O_2$
% Hydrogenated Monoterpenes				**11.36**
% Oxygenated Monoterpenes				**20.57**
% Phenylpropanoids				**67.93**
% Hydrogenated Sesquiterpenes				**0.14**
Total				**100**

* RA: Relative abundance (%); KI: Kovats index.

The analysis of the chemical composition revealed that phenylpropanoids constituted the most abundant group of all identified compounds in the essential oil of *Anethum graveolens*, accounting for 67.93%, followed by monoterpenes divided between oxygenated monoterpenes (20.57%) and hydrogenated monoterpenes (11.36%). Hydrogenated sesquiterpenes were also identified but with a low percentage (0.14%).

Furthermore, the chemical composition of the *A. graveolens* essential oil was rich in ethers (68.04%), followed by ketones with a percentage of 17.57%. We also note the presence of hydrocarbons (11.5%) and alcohols (2.84%). However, aldehydes were nearly absent (0.05%) (Figure 1).

The essential oil extracted from the seeds of *A. graveolens* was mainly composed of (E)-anethole (38.13%), estragole (29.32%), fenchone (17.21%), and α-pinene (7.37%), while other compounds were present in smaller amounts, such as linalool (2.68%) and limonene (1.24%) (Table 4 and Supplementary Figure S2).

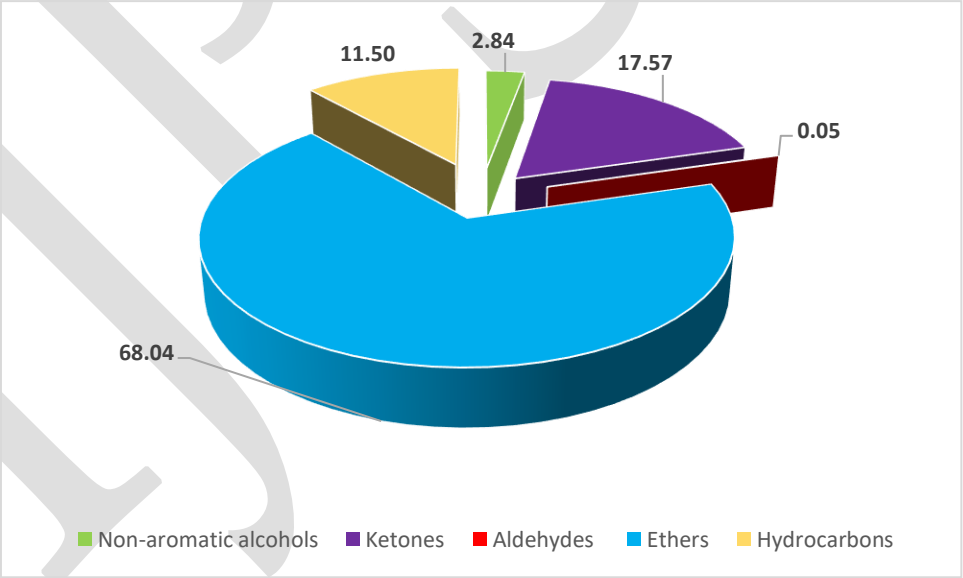

Figure 1. Distribution of the main chemical groups in the essential oil of *A. graveolens*.

Data analysis showed that our A. graveolens essential oil varies chemically from other sources' reported oils, with quantifiable and qualitative variances in individual components. It was our observation that the plant under study had a fascinating chemical polymorphism.

The chemical composition of dill essential oil has been the subject of little research in Morocco. Twelve chemicals, including almost all of the essential oil derived from seeds in southern Morocco, were isolated by Znini et al. [20]. The most abundant of these were carvone (43.5%), dillapiole (26.7%), and limonene (15.4%). Along with it, chromatographic and

The main components of dill essential oil were found to be dillapiole (44.01%), D-limonene (19.47%), and carvotanacetone (13.33%), according to spectrophotometric investigations carried out by El-Sayed et al. [17] on the oil extracted from Egyptian seeds. Snuossi et al. [22] found 24.0% carvone, 25.7% piperitone, 20.6% limonene, 8.0% dillapiole, 4.9% trans-dihydrocarvone, and 4.4% camphor in Tunisia.
The primary components of essential oil from French dill grown in Europe are limonene (48.05%), carvone (37-94%), cis-dihydrocarvone (3.5%), and trans-carvone (1.07%). The number 23. In their analysis of Serbian dill essential oil, Kostić et al. [24] found that oxygenated monoterpenes made up the majority of the composition (52.79%), whereas phenylpropanoids were completely absent. The second group included a significant amount of carvone (42.47%), limonene (29.04%), and α-phellandrene (13.12%). Aati et al. [25] discovered that essential oils isolated from seeds using the Headspace solid-phase microextraction process were high in monoterpenes (65.1%). This was done in an Asian and Saudi Arabian context.
An analysis of its chemical composition revealed that anethole made up 33.3% of the total, limonene 30.8%, carvone 17.7%, and trans-dihydrocarvone 12.2%. According to a research, the essential oil of Iranian dill includes the following compounds: linalool (63.41%), δ-pinene (3.97%), δ-terpinene (4.27%), p-cymene (3.35%), geranyl acetate (3.32%), octyl butyrate (3.3%), and Σ-pinene (3.23%). [26]. Phellandrene (34.19%), carvone (23.67%), limonene (21.47%), α-terpineol (5.58%), and para-cymene (5.50%) were identified as the primary components of this species in the same country as Najafzadeh et al. [14]. Among the essential oils investigated in China, the most important ones are D-carvone (40.36%), D-limonene (19.31%), apiole (17.50%), α-pinene (6.43%), 9-octa-decenoic acid (9.00%), and 9,12-octadecadienoic acid (2.44%) [21]. Similarly, in their study on this species' essential oil, Kaur et al. [9] found that carvone, limonene, camphor, and dihydrocarvone were the main compounds in India, with butyl acetate, myrcene, anethole, α-pinene, and aneth ether as minor compounds.
A number of factors, including the plant's developmental stage, the growing medium, and the targeted plant portion, influence the reported components among research.

2.4. Screening for Plant Biochemicals

Using specialized revealing reagents, phytochemical assays were performed on several extracts obtained from A. graveolens seeds. Table 5 displays the findings of the phytochemical screening.
Polysaccharides, reducing sugars (glucose and fructose), proteins, and lipids were abundant in this species' main metabolites, which came in varying amounts. Also established were the existence of secondary metabolites such as tannins, triterpenes, oses and holosides, leuco-anthocyanins, mucilages, and flavonoids. But saponins and alkaloids weren't there.
Our findings are in agreement with those of El Mansouri et al. [27], who found that dill seeds from Southern Morocco contain an abundance of tannins and flavonoids but no saponins. It is worth noting that Kaur et al. [9]also found phenolic substances, flavonoids, tannins, and terpenoids.

Table 5. Results of phytochemical tests conducted on extracts of *A. graveolens* seeds.

Chemical Group		*A. graveolens*
Polysaccharide		starch
Reducing sugars		+
Protein	**Biuret reaction**	+
	Xanthoprotein reaction	+
Lipids (Lieberman Burchard reaction)		+++
Tannins		+++
Catechic tannins		++

Gallic tannins	++
Flavonoids	++
Leucoanthocyanins	++
Saponosides	-
Alkaloids	-
Reducing Compounds	++
Oses and holosides	++
Mucilages	++
Sterols and triterpenes	++

+++ Very abundant ; ++: abundant; + weak; - absent.

2.4. Phenolic Compound Yields of Extracts

We were able to determine the yield of several phenolic compounds found in the plant under investigation by extracting them. The extracts included ethanol, aqueous, and decocted extracts. The yield was calculated as a percentage relative to 30 g of the plant material that had been dried and powdered. The findings are depicted in Figure 2.

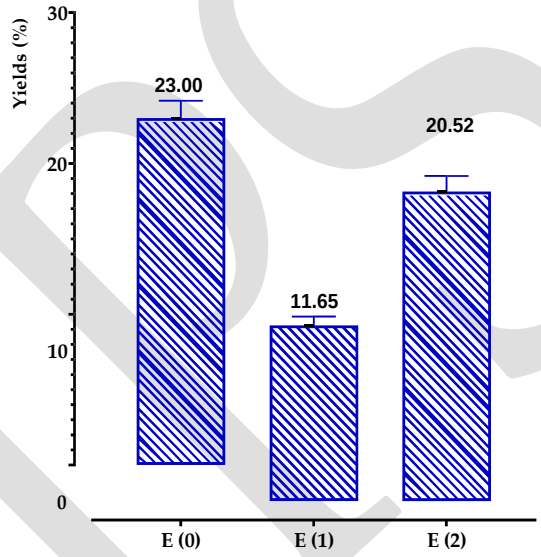

Figure 2. Yields of extracts obtained from *A. graveolens*.

The results obtained showed that extraction yields depended both on the extraction solvent and the extraction method. Indeed, the average extraction yields of phenolic compounds were more or less variable and were higher in the decocted (23.00% ± 0.04) and aqueous extracts (20.52% ± 0.006) than in the ethanol extract (11.65% ± 0.003).

We observed a propensity for water to extract a greater number of chemicals compared to ethanol. This phenomenon may be attributed to the inherent property of water as a highly polar solvent, which has the ability to selectively extract a diverse array of molecules. This includes a substantial quantity of non-phenolic substances, such as sugars and proteins.

2.5. Content of Phenolic Compounds, Flavonoids, and Condensed Tannins

Figure 3 displays the outcomes acquired through the use of a UV–visible spectrophotometer pertaining to the concentrations of total phenolic components and flavonoids in extracts derived from *A. graveolens* seeds. Based on the observed data, it seemed that the amounts of these compounds exhibited significant variation between different extracts. The ethanolic extract recorded the highest quantities of phenolic compounds, flavonoids, and tannins at approximately 52.65 ± 0.22 mg GAE/g of extract, 35.58 ± 2.79 mg QE/g of

extract, and 0.090 mg CE/g of extract, respectively, followed by the aqueous extract noting values of 39.72 ± 0.00 mg GAE/g of extract, 13.79 ± 0.63 mg QE/g of extract, and 0.075 ± 0.002 mg CE/g of extract. Meanwhile, the decoction procedure produced the lowest quantities of the tested molecules; notably, 23.35 ± 0.66 mg GAE/g of extract for phenolic compounds, 9.40 ± 0.51 mg QE/g of extract for flavonoids, and 0.046 ± 0.003 mg CE/g of extract for tannins. The results we obtained are significantly higher than those published by El Mansouri et al. [27]. Our research showed that the decoction had higher quantities of phenolic compounds and flavonoids but a somewhat reduced tannin content compared to a previous study. El Mansouri et al. [27], reported that the dill seed decoction had polyphenol and tannin concentrations of 6.16 mg GAE/g of extract and 0.21 mg CE/g of extract, respectively. This discrepancy underscores the fluctuation in phytochemical composition caused by factors such as geographic source, extraction procedure, and analytical methodologies.

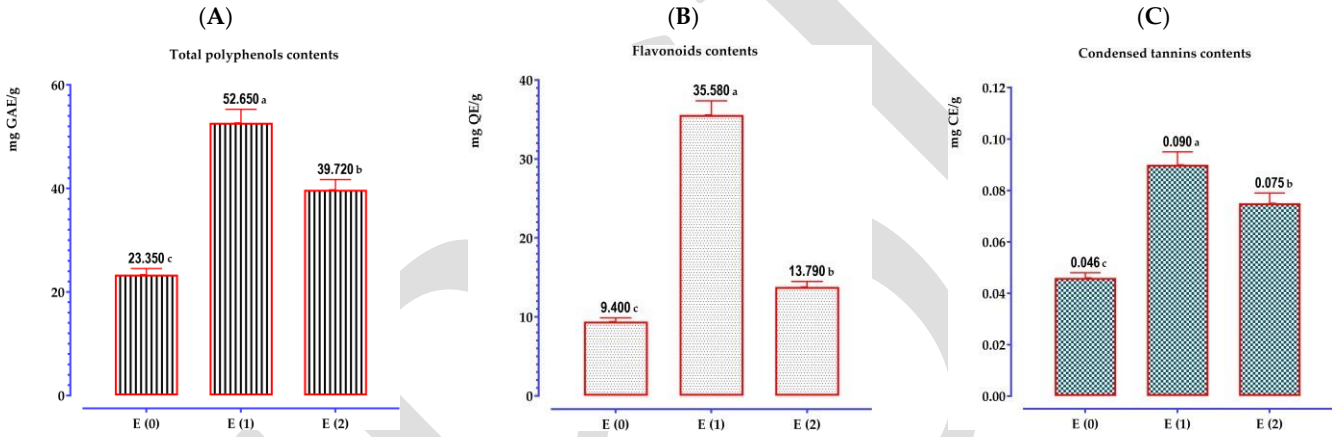

Figure 3. Contents of total polyphenols (**A**), flavonoids (**B**), and condensed tannins (**C**) in extracts from *A. graveolens* seeds. The values are means ± SD. Results with different superscripts are significantly different from each other ($p < 0.05$).

2.6. Chromatographic Analysis by HPLC/UV-ESI-MS of the Extracts

The chromatographic profile, depicted below (Supplementary Figure S3), illustrates the peaks of compounds derived from the decoction of *A. graveolens* seeds, along with their retention times and relative abundances.

Using analytical and spectral data in negative and positive modes, we identified 38 compounds whose names and molecular formulas are presented in Table 6.

Table 6. List of compounds identified by HPLC/UV-ESI-MS in the decoction E (0) of *A. graveolens* seeds.

N°	RT	Area (%)	Molecules	Structure	Classes	Exact Weights	$[M-H]^-$ (*m/z*)	$[M+H]^+$ (*m/z*)	Fragment Ions (*m/z*)
1	4.05	1.8	Medioresinol	$C_{21}H_{23}O_7$	Flavonoid	388	387		207-179
2	4.23	1.75	Caffeic acid	$C_9H_8O_4$	Phenolic acid	180		181	181-163-145-139-114
3	4.33	2.47	Cinnamic acid	$C_9H_8O_2$	Phenolic acid	148	147		119-103-93
4	4.51	1.21	Scopoletin	$C_{10}H_8O_4$	Coumarin	192	191		176-148-104
5	4.75	3.58	Pimelic acid	$C_7H_{12}O_4$	Fatty acid	160	159		115-97
6	5.34	0.53	Retusin	$C_{19}H_{18}O_7$	Flavonoid	358	357		357-342-327-312-297
7	8.39	0.60	Syringic acid	$C_9H_{10}O_5$	Phenolic acid	198	197		179-135-123
8	8.53	1.30	Carnosic acid	$C_{20}H_{27}O_4$	Diterpene	332		333	333-287
9	8.96	12.35	Umbelliferone	$C_9H_6O_3$	Coumarin	162	161		133-106
10	9.00	8.36	Biotin	$C_{10}H_{16}N_2O_3S$	Vitamin	244		243	297-228-174-130

11	9.24	4.21	Coumarin	$C_9H_6O_2$	Coumarin	146		147	147-103
12	9.48	1.34	Kaempferide	$C_{16}H_{12}O_6$	Flavonoid	300	299		217-149-107
13	9.91	11.23	3-Hydroxyflavone	$C_{15}H_{10}O_3$	Flavonoid	238	237		237-135-101
14	10.15	8.95	Rosmanol	$C_{20}H_{26}O_5$	Polyphenol	346	345		243-197-147
15	10.78	3.40	Homovanillic acid	$C_9H_{10}O_4$	Other	182	181		137-123-108
16	11.08	3.35	kaempferol	$C_{15}H_{10}O_6$	Flavonoid	286	285		201-165-151-117
17	11.37	3.56	Methyl rosmarinate	$C_{19}H_{18}O_8$	Polyphenol	374		375	375-181-137
18	11.55	0.98	Chlorogenic acid	$C_{16}H_{18}O_9$	Phenolic acid	354	353		191-179
19	12.33	0.55	Apigenin 7-rhamnoside	$C_{21}H_{20}O_9$	Flavonoid	416		417	417-271-243-229
20	12.71	1.02	Quercitine 7-glucuronide	$C_{21}H_{18}O_{13}$	Flavonoid	478	477		431-301-175
21	12.99	0.42	Epicatechin gallate	$C_{22}H_{18}O_{10}$	Polyphenol	442	441		289-169-125
22	13.72	1.26	Rhamnetin	$C_{16}H_{12}O_7$	Flavonoid	316	315		300-179-165-151
23	13.92	0.42	Riboflavin	$C_{17}H_{20}N_4O_6$	Vitamin	376	375		375-255-243-241
24	14.11	1.29	Quercetin-3-O-galactoside	$C_{21}H_{20}O_{12}$	Flavonoid	464		465	465-427-303-91
25	14.80	1.29	Quercetin 3-O-rhamnoside	$C_{21}H_{20}O_{11}$	Flavonoid	448	447		301-300-284
26	15.25	1.67	δ-tocopherol	$C_{27}H_{46}O_2$	Vitamin	402	401		385-135
27	15.73	3.85	trans-caftaric acid	$C_{13}H_{12}O_9$	Phenolic acid	312	311		249-203-179-149
28	16.10	1.03	3-Feruloylquinic acid	$C_{17}H_{20}O_9$	Phenolic acid	368	367		293-209-193-173
29	16.60	0.56	Quercetin 3,3′-dimethyl ether	$C_{17}H_{14}O_7$	Flavonoid	330	329		314-301-285-270
30	17.35	1.62	Rosmarinic acid	$C_{18}H_{16}O_8$	Phenolic acid	360		361	181-163-145-135-117
31	19.06	1.23	Apigenin	$C_{15}H_{10}O_5$	Flavonoid	270	269		227-159-121-105
32	20.26	0.78	Apigenin-7-glucoside	$C_{21}H_{20}O_{10}$	Flavonoid	432	431		431-385-268-240-151-107
33	20.41	0.80	Folic acid	$C_{19}H_{19}N_7O_6$	Vitamin	441			311-267-224-175
35	21.43	4.91	Emmotin H	$C_{15}H_{16}O_3$	Sesquiterpenoid	244	243		243-228-200-184
36	23.74	0.47	caffeoyl-feruloyltartaric acid	$C_{23}H_{20}O_{12}$	Phenolic acid	488	487		487-443-293
37	25.35	3.37	1-Caffeoyl-beta-D-glucose	$C_{15}H_{18}O_9$	Polyphenol	342	341		341-179-135
38	25.76	0.45	Ascorbyl palmitate	$C_{22}H_{38}O_7$	Other	414		415	415-371-115

The decoction findings showed that the dill extract contains molecules with a wide variety of structures. Indeed, we found many compounds; the most important of them were two coumarins, umbelliferone (12.35%) and coumarin (4.21%), along with a 3-hydroxyflavone flavonoid, rosmanol (8.95%), biotin (8.36%), a sesquiterpenoid, and emmotin H (4.91%). One of the most important methods for determining chemical structures is electrospray ionization-mass spectrometry, or ESI-MS. Fragmentation in both positive and negative ion modes enables the study of each component.

The loss of a proton (H^-) caused the formation of the [M-H]− ion, which was discovered at 8.96 min in the mass spectrometer and was visible at m/z = 161 in the ESI-MS spectrum of umbelliferone. In addition, the typical coumarin structure was characterized by the separation of an acetate (CH3CO) group and a carbon monoxide (CO) group, as shown by the major fragments found at m/z = 133 and 106, respectively. Within the same framework, 3-hydroxyflavone (C15H10O3, M = 238) displayed a [M-H]·⁚· ion at m/z = 237, which emerged at 9.91 min. It was accompanied by significant fragments at m/z = 237, 135, and 101, which indicate the fragmentation of the

the flavonoid structure, which causes the liberation of a CO group and a C5H4O2 piece. Also, after 10.15 minutes, rosmanol showed a $[M-H]^-$ ion at m/z = 345, with significant pieces at m/z = 243 and 197, which is indicative of the typical polyphenolic structure fragmentation. Further evidence of biotin's specific fragmentation may be seen by looking for a [M+H]+ ion at m/z = 243, which emerged at 9.00 min, along with fragments at m/z = 297, 228, 174, and 130. The ion at m/z = 297 may be the consequence of a portion of the biotin's side structure being lost, maybe including a valerate group or a portion of the imidazole. It is possible that the fragment at m/z = 228 is the end product of a C3H8NS group, which includes nitrogen and part of the thiol group. Lastly, the ion at m/z = 174 might be the consequence of a C4H6NO2 group being lost, most likely from a valeric acid or imidazole section.
Likewise, the sesquiterpenoid structure of emmotin H (C15H16O3, M = 244) was characterized by fragments at m/z = 243, 228, 200, and 184, as well as a $[M-H]^-$ ion at m/z = 243, which was detected at 21.43 min. Consistent with negative mass spectrometry techniques, the ion at m/z = 243 was identified as the parent $[M-H]^{\cdot\cdot}$ ion of the emmotin H molecule, showing that a proton was lost during ionization. It is common for sesquiterpenoids to exhibit the dissociation of a CH2 (methylene) group, which may explain the fragment at m/z = 228, among other things. Also, the fragment at m/z = 200 could point to a bigger break in the carbon chain, such the splitting of an alkene or any other functional group. The ion at m/z = 184, which is the last one, may have formed when the sesquiterpenoid skeleton was further fragmented, probably by losing a simpler structure.
The last compound, coumarin (C9H6O2, M = 146), displayed a [M+H]+ ion at m/z = 147, which was detected at 9.24 min. Along with this, a major fragment at m/z = 103 denoted the structure's characteristic fragmentation caused by the loss of a CO group.
Our findings corroborate those of earlier research that has shown how abundant these compounds are in dill seeds. Hydromethanolic extracts of Romanian dill seeds included quercetin, kaempferol, and umbelliferone, according to Bota et al. [28]. In a similar vein, Mashraqi et al. [29] found flavonoids and phenolic acids in Saudi dill, including apigenin, quercetin, rosmarinic acid, caffeic acid, cinnamic acid, and chlorogenic acid. Erdogan et al. [30] also found vanillic acid and rosmarinic acid in abundance in Turkish dill seeds, in addition to these chemicals. In addition, Meena et al. [31] found that dill seeds contain vitamin B1 and vitamin B2.
There is a wealth of information available about the pharmacological effects of coumarins, particularly umbelliferone [32]. Sunscreen agents like this coumarin also have anti-inflammatory, antioxidant, antibacterial, antihyperglycemic, molluscicidal, and anticancer properties [33]. Due to their strong antioxidant activity, apigenin, kaempferol, and quercetin—flavonoids renowned for their different pharmacological effects—are utilized as dietary supplements. They offer a broad variety of biological actions, as shown in many preclinical investigations [34–37]. These include anti-inflammatory, antibacterial, anticancer, and cardioprotective effects. Cancer, cardiovascular disease, hepatotoxicity, neurotoxicity, and viral infections are only a few of the serious pathological conditions that phenolic acids have been shown to alleviate in clinical trials [38–41].
Our study's chemical composition of dill seed extract verifies its use in traditional medicine while also explaining its many pharmacological effects shown in the aforementioned studies. As shown in Supplementary Figure S4, the main compounds discovered in A. graveolens seeds are represented by their chemical structures.

2.7. Antioxidant Activity of A. graveolens Essential Oil and Extracts

2.7.1. Antioxidant Activity of Essential Oil Using DPPH

The results obtained showed a concentration-dependent variation in the inhibition of DPPH* radicals by the *A. graveolens* essential oil. According to the IC_{50} values grouped in Figure 4, the standard antioxidant power of butylated hydroxytoluene (BHT) exceeded that of Dill. Indeed, the latter was considered less effective in reducing free radicals with an IC_{50} equal to 9.02 mg/mL.

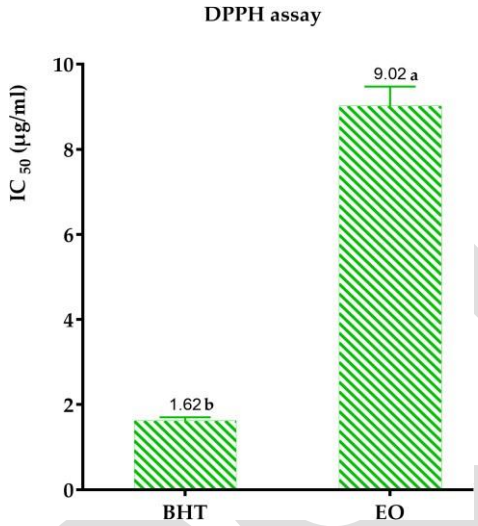

Figure 4. IC_{50} values of *A. graveolens* and the standard antioxidant BHT using the DPPH method.The results with different letters are significantly different from each other ($p < 0.001$).

Several prior investigations have documented this finding. As an example, using the DPPH method, Kaur et al. [9] found that compared to the standard ascorbic acid (IC50 = 0.04 mg/mL), the essential oil of Indian dill (consisting primarily of carvone (41.15%), limonene (23.11%), camphor (9.25%), and dihydrocarvone (3.75%)) had low antioxidant activity (IC50 = 0.65 mg/mL). The scientists concluded that the presence of polar molecules was responsible for this antioxidant potency. The DPPH technique was also used by Osanloo et al. [42] to determine that Iranian dill essential oil has minimal antioxidant activity. The oil's main components include α-phellandrene (26.75%), p-cymene (24.81%), carvone (10.77%), dill ether (9.78), and cis-sabinol (3.61%). Anise, which is mostly made of anethole (96.40%), has lower antiradical activity than dill essential oil, which is 45.24 and 45.90 percent limonene and carvone, respectively, according to a Serbian research [43]. According to Stanojević et al. [44], a concentration of 29 mg/mL for 60 minutes inhibited 79.62% of DPPH radicals in Serbian dill essential oil, which is mostly constituted of carvone (85.9%), limonene (5.1%), and cis-dihydrocarvone (3.0%).
It is the interplay of essential oils' chemical components, which may work either synergistically or antagonistically, that determines their antioxidant activity. Due to their increased reactivity with peroxyl radicals, EOs containing volatile phenolic compounds have a strong antioxidant effect. Additionally, phenylpropanoids made up the majority of the dill essential oil (67.93%) in our study. The antioxidant properties of phenylpropanoids have so been shown in a number of prior investigations [45]. The investigated EO showed modest antioxidant activity; it was constituted of trans-anethole (38.13%), estragole (29.32%), and fenchone (17.21%). The lack of antioxidant activity has been previously observed by Donati et al. [46]. The antioxidant activity of trans-anethole and estragole was assessed by these researchers utilizing the DPPH and FRAP techniques. Their findings indicate that both compounds have modest antioxidant capacity. Senatore et al. [47] also found that compared to the gold standard, Trolox, anethole has a worse capacity to scavenge DPPH free radicals and decrease ferric ions.
Also, the DPPH technique was used to assess the antioxidant activity of the essential oil of I. verum, which is mostly comprised of phenylpropanoids (92.2%), by Luís et al. [48]. Essentially, the authors discovered that the IC50 (3.46%) of this EO, which is rich in trans-anethole (88.5%), is

gallic acid's concentration (0.20%) is roughly seventeen times lower. I. verum EO seems to have a much reduced antioxidant potential when contrasted with the more common gallic acid. In addition, DPPH (1,1-diphenyl-2-picrylhydrazyl) experiments were used to study the antioxidant activity of the essential oil of Indian dill. Remarkably, with concentrations ranging from 5 to 25 µL, the findings demonstrated considerable antioxidant activity with inhibition percentages ranging from 26.1% to 43.62% [49]. Furthermore, estragole's antioxidant potential was shown by Coêlho et al. [50] using DPPH and ABTS techniques; nevertheless, it is still lower than Trolox's. El Omari et al. [51] used the FRAP technique to determine that fenchone has a stronger reducing capacity than camphor and Lavandula stoechas essential oil. Similarly, fenchone's antioxidant effects have been brought to light by Singh et al. [52]. While prior research has shown that trans-anethole, estragole, and fenchone have antioxidant potential, the minor compounds in the studied dill essential oil are also responsible for its moderate antioxidant activity. These compounds may have synergistic or antagonistic effects, depending on the situation.

2.7.2. Antioxidant Activity of Extracts

Based to the results presented in Figure 5, the antioxidant effects of extracts from A. graveolens are shown. The IC_{50} values noted for ascorbic acid and BHA, used as reference compounds by the DPPH and FRAP methods, were significantly lower than those of the extracts, indicating a high antioxidant activity of the standards.

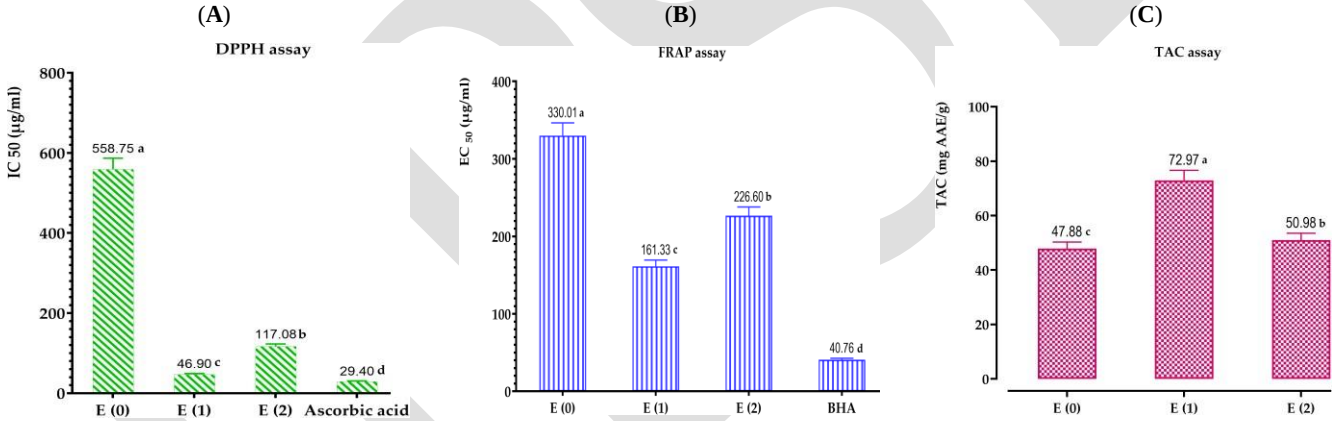

Figure 5. Antioxidant effects of extracts of *A. graveolens* by DPPH (**A**), and FRAP methods (**B**), and CAT (**C**). Mean values ± standard deviations of determinations performed in triplicate are reported; Means are significantly different ($p < 0.001$).

Additionally, we can observe that the nature of the extraction solvent significantly affects the antioxidant activity. Notably, the ethanolic extract, which has shown high contents of polyphenols, flavonoids, and condensed tannins, has proven to be the most active, possessing a powerful antioxidant potential compared to the aqueous extract and decoction.

Moreover, all the tests have allowed us to highlight higher anti-radical ferric and molybdenum ion-reducing activities in the ethanolic extract than in the aqueous extract and decoction. Specifically, the IC_{50} value of this extract reaches 46.90 ± 0.73 µg/mL via the DPPH method, an EC_{50} equal to 161.33 ± 6.18 µg/mL via the FRAP method, and a total antioxidant capacity of 72.97 ± 0.71 mg EAA/g E.

Furthermore, for the aqueous extract, its ability to scavenge DPPH free radicals is superior to that of the decoction. This fact is confirmed by a lower IC_{50} of the aqueous extract (IC_{50} = 117.08 ± 0.16 µg/mL) compared to that of the decoction (IC_{50} = 558.75 ± 4.07 µg/mL). Similarly, for the FRAP and TAC methods, the aqueous extract indicated a higher capacity to reduce ferric and molybdenum ions than the decoction; the EC_{50} value was

226.60 ± 11.73 µg/mL, and the total antioxidant capacity reached 50.98 ± 0.2 mg EAA/g E. In contrast, the decoction had an EC_{50} of 330.01 ± 3.09 µg/mL and a total antioxidant capacity of 47.88 ± 1.73 mg EAA/g E.

Moreover, the difference in the antioxidant activity of the extracts is primarily related to the contents of polyphenols, flavonoids, and other aromatic compounds present. Based on our analysis of the phenolic compound assay results, we have discovered that the examined extracts contain substantial quantities of phenolic compounds. The ethanolic extract exhibits the highest levels of polyphenols, flavonoids, and condensed tannins, surpassing the aqueous extract and the commonly used decoction in traditional medicine.

Furthermore, with the help of the results from the chromatographic analyses conducted using HPLC/UV-ESI-MS for the decoction of dill seeds, we have identified a diverse chemical richness in its chemical profile, reflected by the presence of several chemical families such as coumarins, flavonoids, phenolic acids, and terpenoids. Its main compounds are umbelliferone (12.35%), 3-hydroxyflavone (11.23%), rosmanol (8.95%), vitamin B7 biotin (8.36%), emmotin H (4.91%), and coumarin (4.21%).

The antioxidant potential of *A. graveolens* seeds has been verified by several researchers in the literature. Specifically, Basavegowda et al. [53] have observed strong antioxidant activities of the methanolic extract of dill seeds from India. They have indicated, via the three radical scavenging methods of DPPH, hydroxyl, and nitric oxide, IC_{50} values of 19 ± 0.94, 28 ± 0.36, and 36 ± 0.64 µg/mL, respectively. Moreover, Al-oqail et al. [16] have shown, using the DPPH and hydrogen peroxide radical scavenging methods, that the methanolic extract of Saudi dill seeds has a considerable antioxidant capacity, with IC_{50} values of 225 and 126.3 µg/mL, respectively. Additionally, these researchers have found, using the FRAP method, that the maximum absorbance of this extract is 1.387 at a concentration of 1 mg/mL. Similarly, the study by El Mansouri et al. [27] has revealed the antioxidant power of the aqueous extract of Moroccan dill seeds using the DPPH, ABTS, and hydroxyl radical scavenging methods, as well as the reducing power using FRAP.

2.8. Correlation between Phenolic Compound Content and Antioxidant Activity of Extracts

The entirety of the previously obtained results highlights the relationship between the phenolic compounds and the antioxidant activity of *A. graveolens*. With this in mind, the linear correlation coefficients were calculated (Table 7).

Table 7. Correlation coefficients (R^2) between polyphenol (PC),flavonoid (FC), tannin content (TC) and antioxidant activity of *A. graveolens* extract.

	PC	FC	TC	DPPH	FRAP	CAT
PC	1	0.907	0.994	0.970	0.990	0.762
FC	0.907	1	0.856	0.982	0.957	0.964
TC	0.994	0.856	1	0.938	0.969	0.969
DPPH	0.970	0.982	0.938	1	0.995	0.896
FRAP	0.990	0.957	0.969	0.995	1	0.845
CAT	0.762	0.964	0.686	0.896	0.845	1

The coefficients varied between 0.686 and 0.990. The total polyphenol contents of the extracts correlated strongly with the DPPH (R^2 = 0.970), FRAP (R^2 = 0.990), and CAT (R^2 = 0.762) tests. Similarly, a positive correlation was observed between the flavonoids and the anti-radical activity, reducing activity, and total antioxidant capacity, with Pearson coefficients of R^2 = 0.982, R^2 = 0.957, and R^2 = 0.964, respectively. The antioxidant activity recorded in our extracts is attributed to their richness in phenolic compounds. However, the condensed tannins are an exception. Although the ethanolic, aqueous, and decoction extracts did not possess high contents, there was a significant correlation in the case of FRAP (R^2 = 0.969), DPPH (R^2 = 0.938), and CAT (R^2 = 0.686). This leads us to deduce that, while the quantity of condensed tannins is an important factor, it is not always sufficient, and

there is another criterion related to condensed tannins that must be considered when interpreting antioxidant power, which is the quality criterion. Additionally, there was a positive linear correlation between the three evaluated antioxidant activities, either by the DPPH test and the CAT test for $R^2 = 0.896$, between the DPPH test and the FRAP test for $R^2 = 0.995$, or between the CAT test and the FRAP test for $R^2 = 0.845$. This observation likely indicates that in the three extracts, the polyphenols, flavonoids, and condensed tannins are the major compounds involved in the anti-radical activity, reducing activity, and total antioxidant capacity.

2.9. Antimicrobial Activity

Tables 8 and 9 present the minimum inhibitory concentrations (MICs), minimum fungicidal concentrations (MFCs), and minimum bactericidal concentrations (MBCs) expressed in mg/mL for the extracts and in µL/mL for the essential oil of *Anethum graveolens* against the tested microorganisms.

Table 8. MICs and MBCs (mg/mL) of *A. graveolens* EO and extracts (ethanolic, aqueous, and decocted).

Bacterial Strains	E (0)			E (1)			E (2)			EO		
	MIC	MBC	MBC/MIC	MIC	MBC	MBC/MIC	MIC	MBC	MBC/MIC	MIC	MBC	MBC/MIC
E. cloacae	50	50	1	>50	>50	-	50	50	1	25	25	1
K. pneumoniae	50	50	1	50	50	1	50	50	1	25	25	1
E. coli	>50	>50	-	>50	>50	-	>50	>50	-	25	25	1
S. aureus	50	50	1	50	50	1	50	50	1	25	50	2
S. epidermidis	>50	>50	-	>50	>50	-	>50	>50	-	50	50	1

Table 9. MIC and MFC of *A. graveolens* EO and extracts (ethanolic, aqueous, and decocted).

Fungal Strains	E (0)			E (1)			E (2)			EO		
	MIC	MFC	MFC/MIC	MIC	MFC	MFC/MIC	MIC	MFC	MFC/MIC	MIC	MFC	MFC/MIC
C. albicans	>50	>50	-	50	50	1	50	50	1	3.125	6.25	2
C. dubliniensis	>50	>50	-	6.25	6.25	1	12.5	12.5	1	3.125	3.125	1
C. tropicalis	>50	>50	-	12.5	12.5	1	25	25	1	6.25	6.25	1
C.parapsilosis	>50	>50	-	12.5	12.5	1	12.5	12.5	1	6.25	6.25	1
A. niger	>50	>50	-	0.78	0.78	1	25	25	1	3.125	3.125	1

The findings show that, with the exception of the inert decoction, the dill extracts and essential oil exhibit potential antifungal efficacy when tested against the four fungi. The MICs and MFCs for the water and ethanolic extracts were 0.78–50 mg/mL. One fungus that showed the greatest sensitivity was Aspergillus niger, which had MICs and MFCs of 0.78 mg/mL. Anti-C. albicans experiments yielded MICs and MFCs as high as 50 mg/mL. Both the ethanolic and water-based extracts have anti-fungal and anti-sporicidal activities against Candida parapsilosis when tested at a dosage of 12.5 mg/mL. Also, out of all the extracts we examined, the ethanolic one showed the strongest antifungal activity. Because of its high levels of polyphenols and flavonoids, it has a great deal of action.
The MICs and MFCs for the essential oil varied from 3.125 to 6.25 µL/mL. The most sensitive fungi, A. niger and C. dubliniensis, had minimum inhibitory concentrations (MICs) and maximum concentrations (MFCs) of 3.13 µL/mL. Candida tropicalis and Candida parapsilosis had the highest 50 µL/mL MICs and MFCs.

It seems that different bacterial strains were susceptible to different amounts of the dill extracts and essential oil when it came to antibacterial action. In particular, the water-based and

At a dosage of 50 mg/mL, decoction extracts exhibited bacteriostatic and bactericidal effects on Klebsiella pneumoniae and Staphylococcus aureus. On top of that, the ethanolic extract showed a comparable effect on all of the examined bacterial strains except the dormant Enterobacter cloacae strain. The three extracts that were examined had no effect on S. epidermidis and wild-type E. coli. At a dosage of 25 µL/mL, the essential oil had the opposite effect and killed the E. cloacae, K. pneumoniae, and wild-type E. coli cultures. While S. aureus and S. epidermidis had higher MBCs of 50 µL/mL, they seemed to be less susceptible. The findings of Kaur et al. [54] are supported by these findings. With minimum inhibitory concentrations (MICs) of 40 and 20 mg/mL, respectively, for Escherichia coli and Staphylococcus aureus, these writers have highlighted the antibacterial activity of an aqueous extract of Indian dill seeds. Essential oils derived from several components of the A. graveolens plant in Saudi Arabia, including the leaves, stems, flowers, and seeds, have antibacterial properties, according to another research. An additional finding from this study is that the essential oil derived from the seeds, which contains 33.3% dillapiole, 30.8% limonene, 17.7% carvone, and 12.2% trans-dihydrocarvone, demonstrated a stronger antimicrobial effect compared to the essential oils derived from the other components against S. aureus, Candida albicans, and Candida parapsilosis [25]. In their study, Basavegowda et al. [53] found that an Indian methanolic extract of dill seeds had an antibacterial activity against E. coli, K. pneumoniae, and S. aureus, with minimum inhibitory concentrations (MICs) of 1250, 833, and 125 µg/mL, respectively. In most cases, the chemical makeup of the essential oil is strongly associated with its antimicrobial effect. In addition, the synergistic effects of the principal components present in an equal proportion, namely (E)-anethole (37.2%), estragole (31.1%), and fenchone (28.5%), have been linked by Mota et al. [55] to the essential oil of Foeniculum vulgare seeds' distinctive antibacterial activity.
Thus, (E)-anethole (38.13%), estragole (29.32%), and fenchone (17.21%) were the three primary compounds found in the essential oil that was subjected to our analysis. These percentages were almost identical. Therefore, the antibacterial action is likely due to the synergistic effects of the main components in this complex combination. It is also possible that the examined essential oil's high ether content (68.04%) and presence of ketones (17.57%) are responsible for its antibacterial ability.

2.10. Protox II Toxicology, Anti-Stress, Anti-Microbial, and Efficacy Assessment of Chemicals Derived from A. graveolens Seed Essential Oil and Water Extract
To establish the efficacy of A. graveolens as a nutraceutical preservative agent and to create therapeutic agents, it is essential to analyze the physicochemical properties of the candidate compounds in addition to its biological attributes. Consequently, the compounds contained in A. graveolens seeds' essential oil and water extract were the subject of an analysis to ascertain their medicinal, pharmacokinetic, and physicochemical properties.
For the purpose of conducting PASS and ADMET prediction studies, the primary compounds found in the essential oil (EO) and water-based extract (umbelliferone, 3-Hydroxyflavone, rosmanol, biotin, emmotin H, cou-marin, trans-caftaric acid, pimelic acid, methyl rosmarinate, homovanillic acid, 1-caffeoyl- beta-D-glucose, and kaempferol) of A. graveolens were chosen for the studies.
An online program called ChemBio-Draw was used to produce the SMILES formats of these compounds [56]. Then, the PASS web prediction tool [57] and the SwissADME and pkCSM [58] web tools were used for simulation. Table 10 displays the results of the ADMET and PASS prediction experiments. Using PASS predictions, we assessed the antioxidant and antibacterial efficacy of the main components isolated from A. graveolens seed EO and pure water extract.
According to our predictions, all of the relevant compounds exhibited high "Pa" values for various activities, such as antioxidants (0.150-0.856), antifungals (0.267-0.717), and antibacterials (0.216-0.587) (Table 10). In addition, these substances exhibited very good anti-bacterial properties, strong antifungal effects, and beneficial antioxidant properties.
For the purpose of assessing the pharmacokinetic characteristics and medicinal similarity of specific substances, the pkCSM and SwissADME websites prove to be invaluable. According to Table 10, all of the compounds that were chosen had high lipophilicity indices, meaning they dissolve well in water. The selected compounds had strong Caco-2 permeability values and good skin permeability (log Kp). With the exception of trans-caftaric acid, the majority of the substances investigated exhibit high intestinal

absorption (HIA > 30%).

Important roles in medication distribution and absorption are played by the P-glycoprotein, or P-gp. The examined essential oil does not include any chemical compounds that inhibit P-gp I or P-gp II, and neither are the primary components of the oil P-gp substrates. On the other hand, we found that three-hydroxyflavone, rosmanol, methyl rosmarinate, homovanillic acid, 1-caffeoyl-beta-D-glucose, and kaempferol are molecules in the water extract that may be P-gp substrates. Furthermore, no other compound could suppress P-gp I activity than rosmanol.

With an SNC score over -3.0, eight of the sixteen isolated chemicals tested were shown to readily pass the blood-brain barrier (BBB). Biotin, emmotin H, coumarin, trans-caftaric acid, pimelic acid, methyl rosmarinate, homovanillic acid, and 1-caffeoyl-beta-D-glucose were notable outliers that did not achieve this threshold. The components of the essential oils under study and 3-hydroxyflavone isolated from the water extract were among the chemicals with poor CNS penetration (log BB > 0.3). A range of -1.533 L/kg to 1.274 L/kg was their tissue volume of distribution (logVDss).

While cytochrome P450 (CYP) enzymes and molecular interactions are vital in the elimination of medications, the primary components of the essential oil and aqueous extract under consideration are not anticipated to have adverse effects when taken orally as a result of drug interactions. The excretion route was predicted using the retinal organic cation transporters 2 (OCT2) and the total clearance of hepatic and renal substrates (CLTOT), both expressed in log mL/min/kg. Good overall clearance values and excretion were seen for all of the phytochemical substances that were examined.

Many factors were investigated to determine the possible toxicity of A. graveolens seed essential oil and water extract, including AMES, hERG channel inhibition, skin sensitization, immunotoxicity, hepatotoxicity, carcinogenicity, mutagenicity, and cytotoxicity. Table 11 shows the results of the investigation, which concentrated on the primary phytochemical components. With a few exceptions, the data showed no discernible harmful consequences. Anethole, biotin, estragole, umbelliferone, 3-hydroxyflavone, and coumarin are some of the chemicals that may have low carcinogenicity and low liver effects. On the other hand, immunotoxicity effects might be shown by rosmanol, trans-caftaric acid, methyl rosmarinate, and 1-Caffeoyl-beta-D-glucose. Lastly, a naturally occurring chemical molecule in the coumarin family called umbelliferone (or 7-hydroxycoumarin) has an LD50 of 10,000 mg/kg and is categorized as predicted toxin class 6. This chemical is present in high concentrations in the water-based extract of the A. graveolens seeds used in the research. Based on these results, the essential oil and water extracts of A. graveolens seeds from southern Morocco are safe to use as nutraceuticals or as an alternative to synthetic preservatives when taken orally at the recommended dosages. But to prove beyond a reasonable doubt that there are no dangers to consumers in the long run, further studies, including rigorous clinical trials, are required.

Table 10. In Silico Analysis of PASS, ADME of Compounds from the Essential Oil, and Decoction of *A. graveolens* Seeds.

Prediction	Parameters	EO 1	EO 2	EO 3	EO 4	D 1	D 2	D 3	D 4	D 5	D 6	D 7	D 8	D 9	D 10	D 11	D 12
PASS Prediction (Pa/Pi)																	
Antioxidant	Antioxidant	0.337/0.018			0.563/0.005	0.641/0.004	0.551/0.005	0.150/0.103	0.286/0.026	0.389/0.013	0.711/0.004	0.260/0.033	0.483/0.007	0.321/0.020	0.751/0.004	0.856/0.003	0.337/0.018
Antimicrobial	Antifungal	0.425/0.045	0.267/0.097	0.439/0.042	0.519/0.027	0.367/0.058	0.639/0.014	0.494/0.032	0.504/0.030	0.440/0.041	0.544/0.024	0.363/0.059	0.474/0.035	0.292/0.084	0.717/0.009	0.495/0.031	0.425/0.045
	Antibacterial	0.264/0.075	0.219/0.102	0.326/0.051	0.398/0.030	0.331/0.049	0.569/0.011	0.357/0.041	0.301/0.060	0.344/0.045	0.303/0.059	0.292/0.063	0.218/0.102	0.216/0.104	0.587/0.010	0.395/0.031	0.264/0.075
ADME Prediction																	
Physiochemical Properties	TPSA (Å²)	9.23	9.23	17.07	0.00	50.44	50.44	86.99	103.73	54.37	30.21	161.59	74.60	133.52	66.76	156.91	111.13
	Molar Refractivity	47.83	47.04	45.64	45.22	44.51	69.94	93.99	69.34	70.37	42.48	70.60	39.31	95.72	46.50	79.13	76.01
Drug Likeness Prediction	Bioavailability Score	0.55	0.55	0.55	0.55	0.55	0.55	0.55	0.56	0.55	0.55	0.11	0.85	0.55	0.85	0.55	0.55
	Synthetic accessibility	1.47	1.28	3.22	4.44	2.56	2.93	5.07	3.38	3.03	2.74	3.45	1.37	3.52	1.49	4.47	3.14
Absorption Parameters Prediction	Water solubility	−2.936	−2.874	−3.097	−3.733	−2.131	−3.683	−3.606	−2	−3.366	−1.517	−2.541	−1.088	−3.17	−2.453	−1.869	−3.04
	Caco2 permeability	1.669	1.41	1.501	1.38	1.206	1.263	1.015	0.698	1.267	1.649	−0.801	0.598	−0.562	0.265	0.05	0.032
	Intestinal absorption (human)	95.592	94.536	95.813	96.041	94.551	94.776	93.407	71.182	96.41	97.344	9.399	72.877	64.776	86.286	50.517	74.29
	Skin Permeability	−1.139	−1.739	−1.872	−1.827	−2.6	−2.775	−2.772	−2.727	−2.93	−1.921	−2.735	−2.735	−2.735	−2.722	−2.74	−2.735
	P-glycoprotein substrate	No	No	No	No	No	Yes	Yes	No	No	No	No	No	Yes	Yes	No	Yes
	P-glycoprotein I inhibitor	No	No	No	No	No	No	Yes	No	No	No	No	No	No	No	No	No
	P-glycoprotein II inhibitor	No	No	No	No	No	No	No	No	No	No	No	No	No	No	No	No
	VDss (human)	0.343	0.401	0.341	0.667	0.032	0.214	0.653	−0.933	0.161	−0.143	−0.919	−1.429	0.75	−1.533	0.141	1.274

Distribution Parameters Prediction	Fraction unbound (human)	0.266	0.213	0.423	0.425	0.432	0.151	0.109	0.58	0.3	0.367	0.472	0.543	0.229	0.467	0.609	0.178
	BBB permeability	0.529	0.601	0.624	0.791	−0.278	0.462	−0.581	−0.679	0.291	−0.007	−1.233	−0.21	−1.454	−0.312	−1.081	−0.939
	CNS permeability	−1.659	−1.74	−1.988	−2.201	−2.741	−1.733	−2.101	−3.541	−2.784	−1.926	−3.93	−3.042	−3.358	−2.723	−3.982	−2.228
Metabolism Parameters Prediction	CYP2D6 substrate	No	No	No	No	No	No	No	No	No	No	No	No	No	No	No	No
	CYP3A4 substrate	No	No	No	No	No	Yes	No	No	No	No	No	No	Yes	No	No	No
	CYP1A2 inhibitor	Yes	Yes	No	No	Yes	Yes	No	No	Yes	Yes	No	No	No	No	No	Yes
	CYP2C19 inhibitor	No	No	No	No	No	Yes	No	No	No	No	No	No	No	No	No	No
	CYP2C9 inhibitor	No	No	No	No	No	No	No	No	No	No	No	No	No	No	No	No
	CYP2D6 inhibitor	No	No	No	No	No	No	No	No	No	No	No	No	No	No	No	No
	CYP3A4 inhibitor	No	No	No	No	No	No	No	No	No	No	No	No	No	No	No	No
Excretion	Total Clearance	0.268	0.332	0.085	0.043	0.706	0.233	0.289	0.368	0.19	0.97	0.449	0.565	0.187	0.246	0.059	0.477
	Renal OCT2 substrate	No	No	No	No	No	No	No	No	No	No	No	No	No	No	No	No

EO1: E-Anethole; EO2: Estragole; EO3: Fenchone; EO4: α-Pinene; D1: Umbelliferone; D2: 3-hydroxyflavone; D3: Rosmanol; D4: Biotine; D5: Emmotin H; D6: Coumarin; D7: trans-Caftaric acid; D8: pimelic acid; D9: Methyl rosmarinate; D10: Homovanillic Acid; D11: 1-Caffeoyl-beta-D-glucose; D12: Kaempferol.

Table 11. In silico analysis of the predictive toxicity (ProTox II) of Compounds from the Essential Oil and Decoction of *A. graveolens* Seeds.

Compounds	AMES Toxicity	hERG I Inhibitor	hERG II Inhibitor	Skin Sensitization	Minnow Toxicity	LD_{50} (mg/kg)	Predicted Toxicity Class	Hepatotoxicity	Carcinogenicity	Immunotoxicity	Mutagenicity	Cytotoxicity
EO1	No	No		Yes	0.869	150	3	Inactive	Active (0.57)	Inactive	Inactive	
EO2	Yes			Yes	1.398	1230	4		Active (0.51)			
EO3	No			Yes	1.366	775	4		Inactive			
EO4	No			No	1.159	3700	5		Inactive			
D1	No	No	No	No	1.714	10,000	6	Inactive	Active (0.64)	Inactive	Inactive	Inactive
D2	Yes		No		1.205	2500	5	Inactive	Inactive	Inactive		Inactive
D3	No		Yes		0.285	450	4	Inactive	Inactive	Active (0.95)		Inactive
D4	No		No		2.183	4000	5	Active (0.41)	Inactive	Inactive		Inactive
D5	No		No		1.329	1600	4	Inactive	Inactive	Inactive		Inactive
D6	No	No	No	No	1.555	196	3	Inactive	Active (0.83)	Inactive	Inactive	Active (0.55)
D7	No		No		4.872	3800	5	Inactive	Inactive	Active (0.97)		Inactive
D8	No		No		2.006	900	4	Inactive	Inactive	Inactive		Inactive
D9	No		No		1.92	5000	5	Inactive	Inactive	Active (0.93)		Inactive
D10	No		No		2.106	1123	4	Inactive	Inactive	Inactive		Inactive
D11	No		No		5.989	5000	5	Inactive	Inactive	Active (0.95)		Inactive
D12	No		No		2.885	3919	5	Inactive	Inactive	Inactive		Inactive

EO1: E-Anethole; EO2: Estragole; EO3: Fenchone; EO4: α-Pinene; D1: Umbelliferone; D2: 3-hydroxyflavone; D3: Rosmanol; D4: Biotine; D5: Emmotin H; D6: Coumarin; D7: trans-Caftaric acid; D8: pimelic acid; D9: Methyl rosmarinate; D10: Homovanillic Acid; D11: 1-Caffeoyl-beta-D-glucose; D12: Kaempferol.

2.10. Molecular Docking

Considering the much-increased in vitro bioactivities shown in the EO and aqueous extract of *A. graveolens* in this work, the compounds discovered using GC/MS and HPLC/UV-ESI-MS were chosen for in silico molecular docking experiments.

The antioxidant, antifungal, and antibacterial activities of the compounds, as well as their potential mechanism of action, were deduced through molecular docking experiments. These deductions were based on the molecular interactions at the atomic level between the compounds and their respective target proteins (1JZQ, 1KZN, 2CAG, 2VEG, 2ZDQ, 3SRW, 3UDI, 4URN, 2CDU, 1OG5, and 3NRZ). The molecular docking study was mostly concentrated on assessing factors such as Van der Waals (VDW) interactions, hydrogen bonds, binding free energy, and carbon–hydrogen (C–H) bonds. The stability of the ligands (chosen molecules) and the docked receptor is determined by the C–H bonds and Pi-sigma interactions, whereas the binding interactions are influenced by hydrogen bonds and Van der Waals (VDW) interactions. Table 12 displays the docking energy binding scores for the binding sites of the target proteins involved in antibacterial activities (1JZQ, 1KZN, 2CAG, 2VEG, 2ZDQ, 3SRW, 3UDI, and 4URN), as well as antioxidant activities (2CDU, 1OG5, and 3NRZ). This study analyzed the Van der Waals interactions, hydrogen bonds, and C–H bonds involving the amino acids found in the binding sites of the selected proteins.

Table 12. Details of the Binding Affinities of Antimicrobial and Antioxidant Target Proteins with Selected Ligands.

Ligands\Targets	1JZQ	1KZN	2CAG	2VEG	2ZDQ	3SRW	3UDI	4URN	2CDU	1OG5	3NRZ
EO1	−5.1	−5.6	−7.1	−4.8	−7.1	−5.8	−4.7	−5.5	−5.6	−5.4	−7.5
EO2	−5.2	−5.6	−6.7	−4.5	−7.0	−5.5	−4.6	−5.3	−5.5	−5.3	−7.0
EO3	−5.6	−4.8	−6.5	−4.6	−6.6	−5.9	−5.0	−4.7	−5.3	−6.0	−6.2
EO4	−5.5	−4.6	−6.0	−4.6	−6.2	−5.6	−4.5	−4.6	−5.0	−5.5	−5.1
D1	−6.0	−6.7	−8.1	−5.8	−8.2	−6.4	−5.8	−6.2	−6.4	−6.3	−8.8
D2	−7.6	−7.7	−9.4	−7.0	−8.4	−8.1	−7.4	−7.5	−7.5	−7.9	−8.8
D3	−8.2	−8.0	−7.2	−7.0	−6.5	−8.6	−8.2	−7.7	−7.3	−8.9	−6.2
D4	−6.3	−6.2	−7.5	−5.3	−7.3	−7.0	−6.0	−6.2	−6.1	−7.1	−7.0
D5	−7.5	−7.5	−9.0	−6.2	−10.0	−8.0	−7.6	−6.3	−7.6	−8.0	−6.2
D6	−5.8	−6.6	−7.7	−5.5	−7.9	−6.3	−5.6	−5.8	−6.4	−6.6	−8.1
D7	−6.8	−7.3	−8.9	−6.8	−9.1	−7.8	−7.2	−6.5	−7.9	−7.3	−7.6
D8	−4.9	−5.2	−5.9	−4.5	−5.8	−4.9	−4.9	−4.9	−5.1	−5.4	−6.6
D9	−7.8	−8.4	−10.2	−7.8	−9.2	−8.4	−8.3	−7.3	−8.0	−8.4	−9.8
D10	−5.5	−6.1	−7.1	−5.4	−7.0	−6.0	−5.5	−5.5	−6.1	−6.0	−7.4
D11	−7.6	−7.6	−9.5	−6.7	−9.8	−8.0	−7.4	−7.0	−7.7	−7.9	−10.0
D12	−8.1	−8.2	−10.0	−6.6	−9.0	−8.5	−8.3	−7.9	−7.7	−8.6	−7.8

EO1: E-Anethole; EO2: Estragole; EO3: Fenchone; EO4: α-Pinene; D1: Umbelliferone; D2: 3-hydroxyflavone; D3: Rosmanol; D4: Biotine; D5: Emmotin H; D6: Coumarin; D7: trans-Caftaric acid; D8: pimelic acid; D9: Methyl rosmarinate; D10: Homovanillic Acid; D11: 1-Caffeoyl-beta-D-glucose; D12: Kaempferol.

The results of our study reveal that among the tested compounds, 3-hydroxyflavone, emmotin H, trans-caftaric acid, methyl rosmarinate, 1-caffeoyl-beta-D-glucose, and kaempferol presented the greatest binding energies with the exploratory proteins. These compounds demonstrated significant interactions with different target proteins involved in antimicrobial and antioxidant activities. In particular, 3-Hydroxyflavone exhibited a marked affinity with the 2CAG protein (−9.4 Kcal/mol) for antimicrobial activity. Similarly, Emmotin H manifested substantial binding energy with the 2ZDQ protein in this

same context (−10 Kcal/mol). Moreover, Caftaric <trans> acid also displayed a strong affinity with the 2ZDQ protein (−9.1 Kcal/mol) for antimicrobial activity.

On the other hand, Methyl rosmarinate revealed significant binding energies with the 2CAG (−10.2) and 2ZDQ (−9.2 Kcal/mol) proteins for antimicrobial activity, as well as with the 3NRZ (−9.8 Kcal/mol) protein for antioxidant activity. Similarly, 1-Caffeoyl-beta-D-glucose presented high affinity with the 2CAG (−9.5 Kcal/mol) and 2ZDQ (−9.8 Kcal/mol) proteins for antimicrobial activity, as well as with the 3NRZ (−10 Kcal/mol) protein for antioxidant activity. Finally, Kaempferol also demonstrated substantial binding energy with the 2CAG protein (−10 Kcal/mol) for antimicrobial activity. These results highlight the promising potential of these bioactive compounds as antimicrobial and antioxidant agents, thus paving the way for future research in the fields of pharmaceutical chemistry and natural products.

The study of interaction types using Discovery Studio revealed that the interactions of 3-Hydroxyflavone with Catalase were associated with hydrogen bonds, Pi-alkyl, Pi-cation, and Pi–Pi-stacked with each of these residues (HIS341, PHE313, VAL125, ALA112, ALA340, ARG51, HIS54, and TYR337, respectively) (Figure 6).

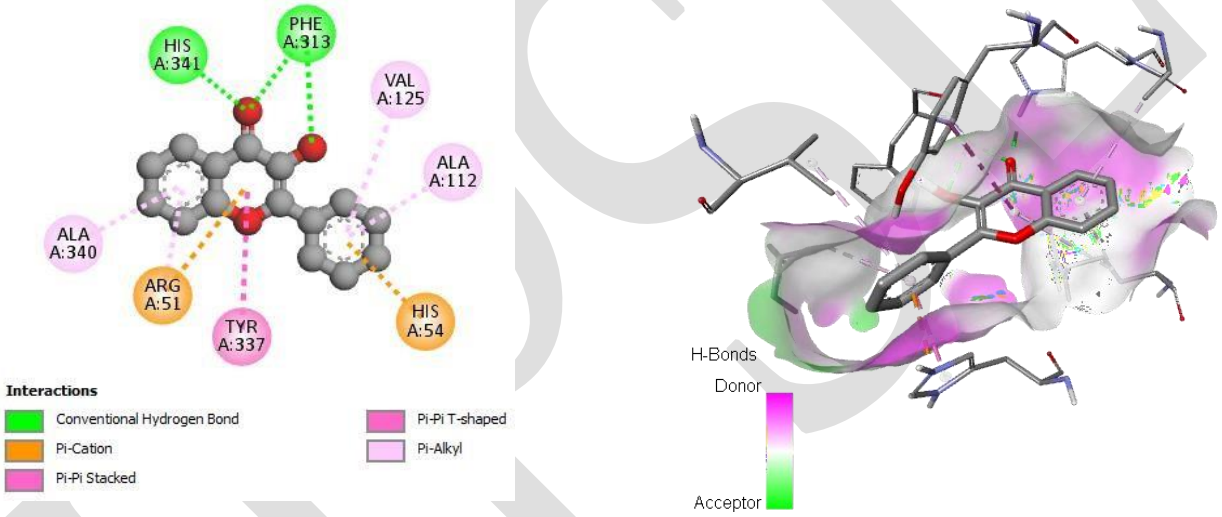

Figure 6. 2D and 3D Interactions of 3-Hydroxyflavone with the 2CAG Target Protein.

This interaction study revealed that in the case of the D-alanine ligase protein, Emmotin H developed hydrogen bonds, Pi–Pi stacking, and Pi–alkyl interactions with each of the residues (LYS153, PHE151, VAL195, and ALA191, respectively) at their binding site on the D-Alanine Ligase (Figure 7).

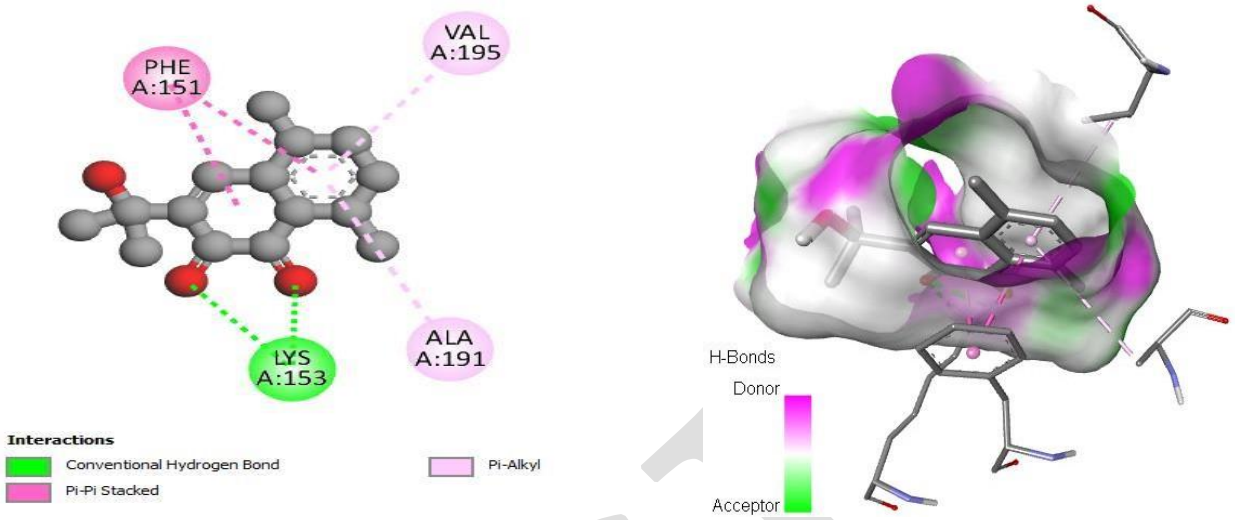

Figure 7. 2D and 3D interaction of Emmotin H with D-Alanin Ligase protein.

Furthermore, in the case of trans-caftaric acid, hydrogen bonds and Pi–Pi stacking interactions were observed with each of the residues (GLU189, ASN281, GLU197, ASP270, GLU282, LYS228, SER160, PHE272, and PHE151) (Figure 8).

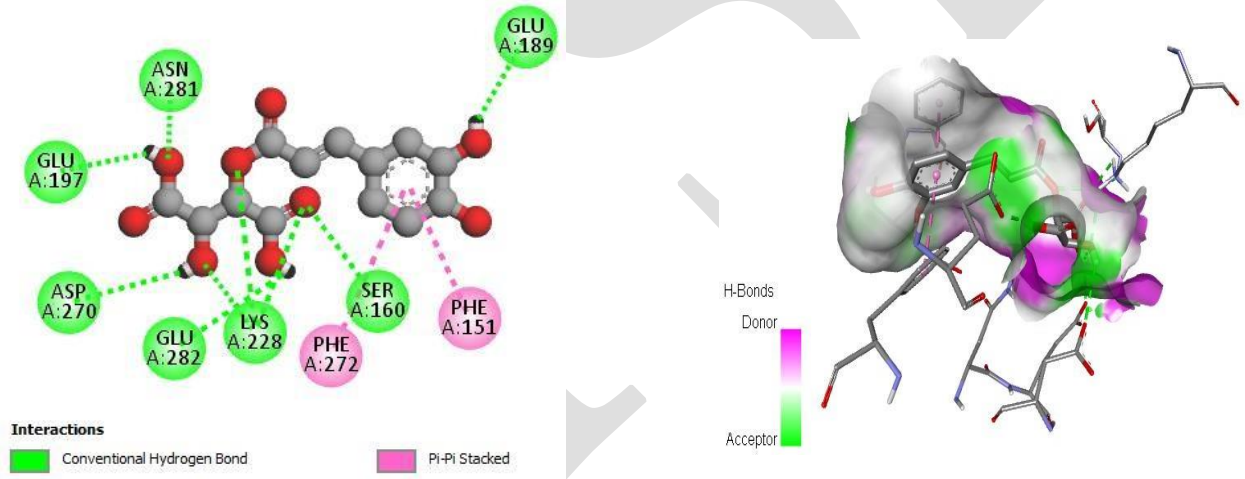

Figure 8. 2D and 3D Interactions of trans-caftaric Acid with the 2ZDQ Protein.

For each of these catalytic residues (ARG344, PHE313, HIS341, ARG91, ARG51, TYR337, HIS54, VAL125, ALA340, and ALA112), the interaction of Methyl rosmarinate with them involved hydrogen bonds, carbon–hydrogen bonds, Pi–Pi stacked interactions, and Pi–alkyl interactions (Figure 9). On the other hand, the interactions of this molecule with D-Alanine ligase were associated with hydrogen bonds, carbon–hydrogen bonds, Pi–cation, Pi–anion, and Pi–Pi stacked interactions with each of the involved residues (GLU199, ARG268, LYS190, LEU192, LYS228, SER160, THR157, GLU282, ASP270, PHE151, and PHE272) (Figure 9). Finally, the interactions of Methyl rosmarinate with 3NRZ were characterized by hydrogen bonds, carbon–hydrogen bonds, Pi–Pi stacked, Pi–Pi-shaped, and Pi–alkyl interactions with each of the concerned proteins (SER1082, GLY799, GLN767, ALA1079, THR1010) (Figure 9).

(A) (2CAG)

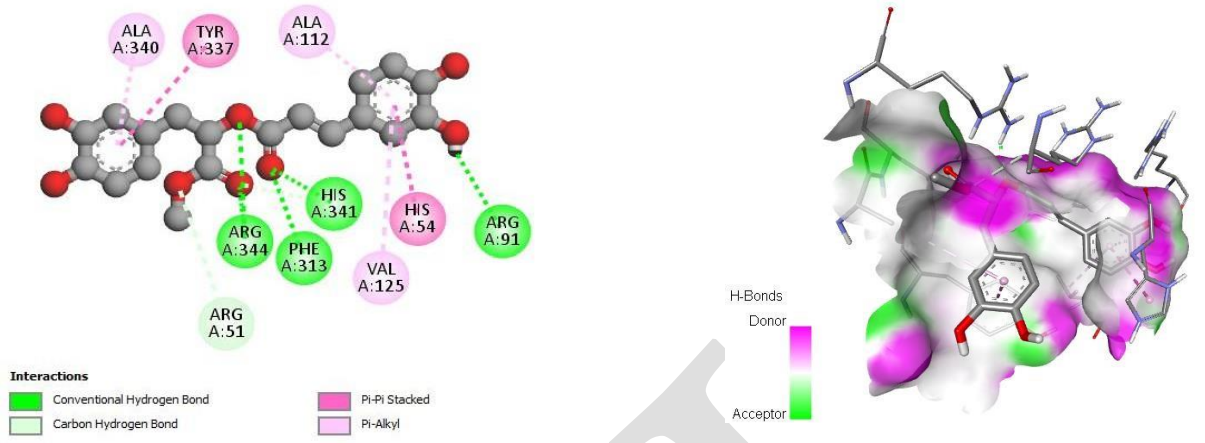

(B) (2ZDQ)

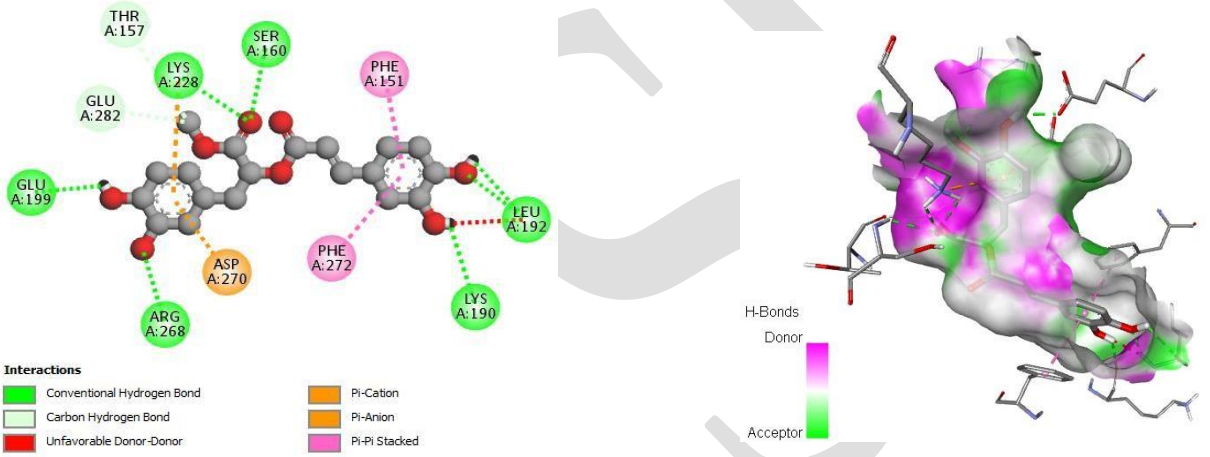

(C) (3NRZ)

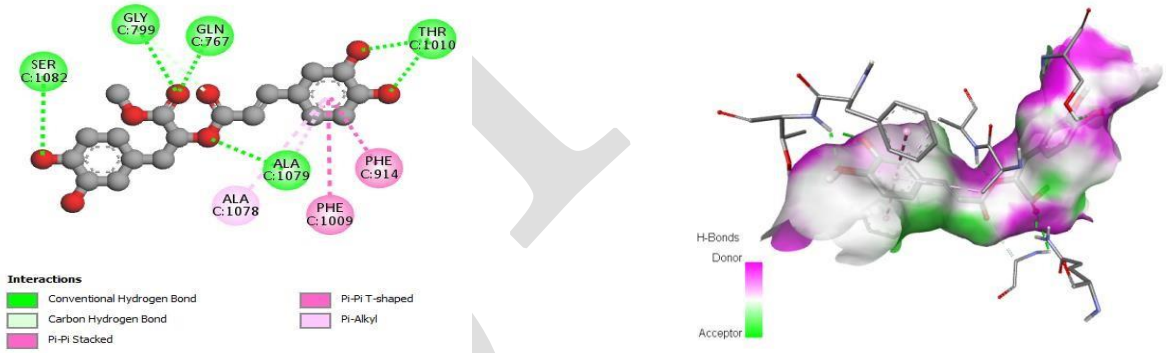

Figure 9. 2D and 3D interaction of methyl rosmarinate with target proteins: (**A**) 2CAG, (**B**) 2ZDQ, and (**C**) 3NRZ.

For each protein (OMT53, ARG344, PHE312, GLY126, ALA312, TYR337, ALA112, HIS54, and VAL125), the interaction of 1-Caffeoyl-beta-D-glucose with catalase was associated with hydrogen bonds, carbon–hydrogen bonds, Pi–sigma interactions, Pi–Pi stacked interactions, and Pi–alkyl interactions (Figure 10). Furthermore, the interactions of 1-Caffeoyl-beta-D-glucose with D-Alanine ligase were characterized by hydrogen bonds, carbon–hydrogen bonds, Pi–Pi stacked interactions, and Pi–alkyl interactions with each of the involved proteins (LYS190, GLU189, ASN281, LYS228, TYR223, ASP270, LYS116, PHE151, PHE272, LEU192, and VAL195) (Figure 10). Finally, the interactions of 1-Caffeoyl-beta-D-glucose with bovine xanthine oxidase were associated with hydrogen bonds, carbon–hydrogen bonds, Pi–Pi stacked, Pi–Pi-shaped, and Pi–alkyl interactions with each of the concerned proteins (PHE798, GLY799,

SER1080, GLU802, THR1010, ALA1079, THR1077, ALA1078, PHE914, and PHE1009) (Figure 10).

(A) (2CAG)

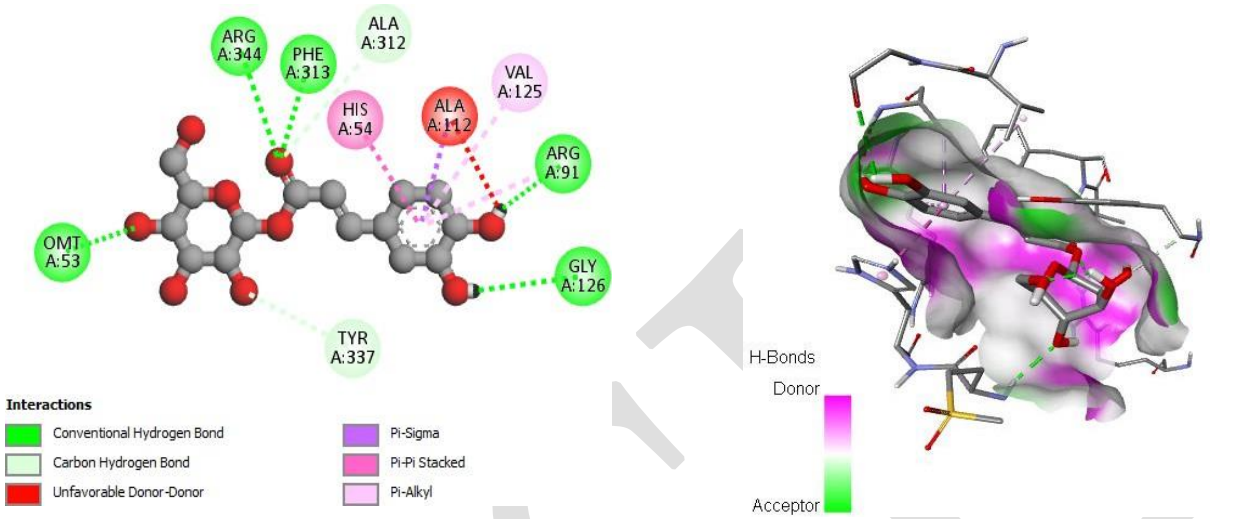

(B) (2ZDQ)

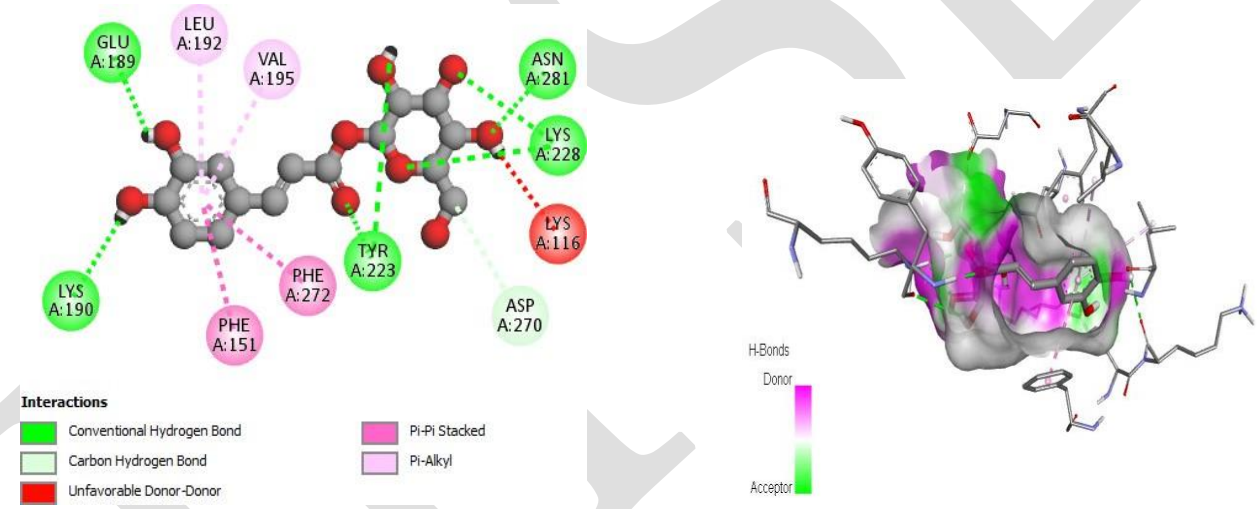

(C) (3NRZ)

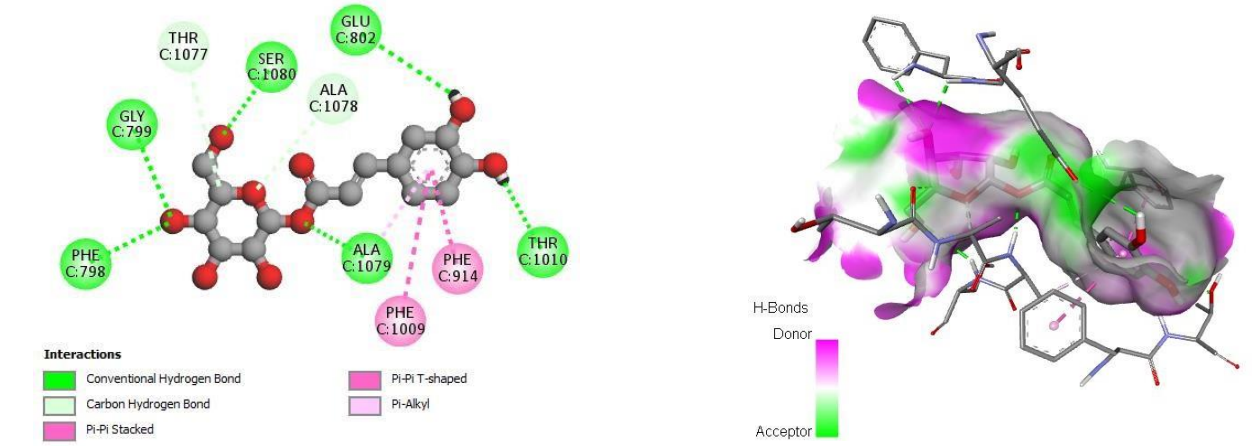

Figure 10. 2D and 3D interaction of 1-Caffeoyl-beta-D-glucose with target proteins: (**A**) 2CAG, (**B**) 2ZDQ, and (**C**) 3NRZ.

In conclusion, the interaction analysis has highlighted that the interactions of Kaempferol with the catalase protein were characterized by hydrogen bonds, carbon–hydrogen bonds, Pi–sigma interactions, Pi–Pi stacked interactions, and Pi–alkyl interactions with each of the protein residues (ARG344, HIS341, PHE313, ALA112, HIS54, ALA340, ARG51, and ARG91, respectively) (Figure 11).

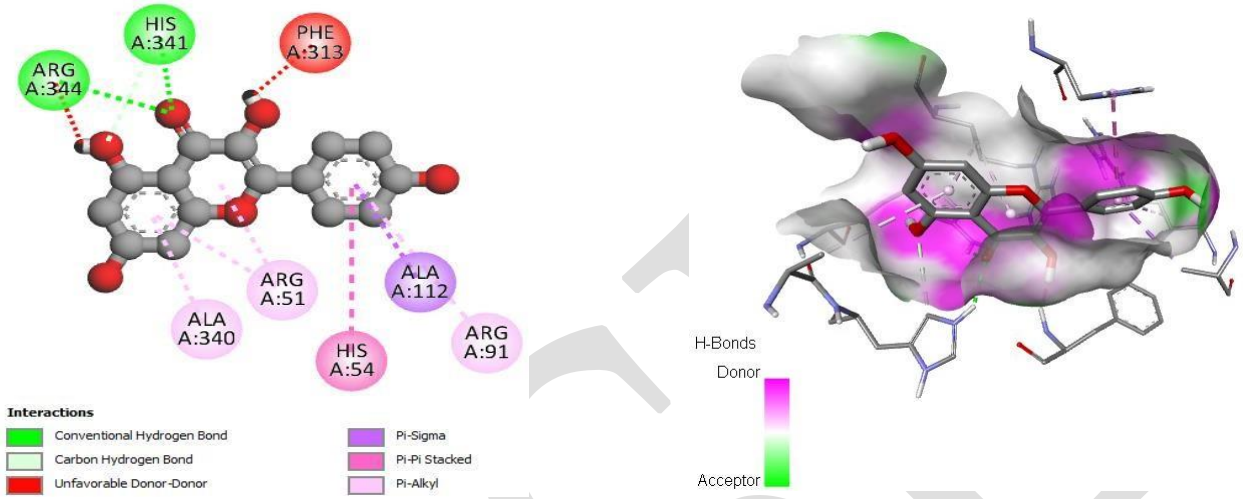

Figure 11. Interaction of 2CAG with kaempferol.

2.11. Molecular Dynamics Simulation

It should be noted that protein targets might experience substantial conformational changes while interacting with pharmacological molecules. To comprehend the internal movements, conformational changes, and stability of protein-ligand complexes, molecular dynamics simulation (MDS) is an excellent method. We can calculate parameters like root-mean-square deviation (RMSD), root-mean-square fluctuation (RMSF), radius of gyration (Rg), number of hydrogen bonds, and binding free energy by analyzing MDS trajectories for the ten complexes. In the case of 3NRZ, there are two complexes, in the case of 2CAG there are four, and in the case of 2ZDQ there are four. Insights into the complexes' structural stability, binding modalities, and binding strengths are provided by these investigations.

The 3NRZ's Structural Dynamics (2.11.1)

The intricate structural dynamics of protein 3NRZ in interaction with methyl-rosmarite and 1-Caffeoyl-beta-D-glucose ligands were examined in our work using molecular dynamics simulations. The nuanced impact of ligand binding on conformational stability of the protein was our target. We zeroed down on a number of metrics to understand the dynamic interaction between the protein and ligands. All of the protein-ligand entities had less spectrum fluctuation, as shown in the RMSD graph in Figure 12. This suggests that their structural dynamics were relatively unaffected during the simulation. The RMSF research looked at how ligand binding affected protein dynamics over 100 ns, and it found that protein-ligand complexes were less flexible and had fewer possible conformational changes. As shown in Figure 12, this indicates that the influence of all complexes on receptor flexibility is modest. In addition, the complexes showed continuous patterns in the Radius of Gyration (RG) profiles, which suggests that the formation is stable. Importantly, examination of hydrogen bonding revealed the creation of many hydrogen bonds in both complexes, highlighting their crucial function in stability maintenance, even when the ligands dissociate.

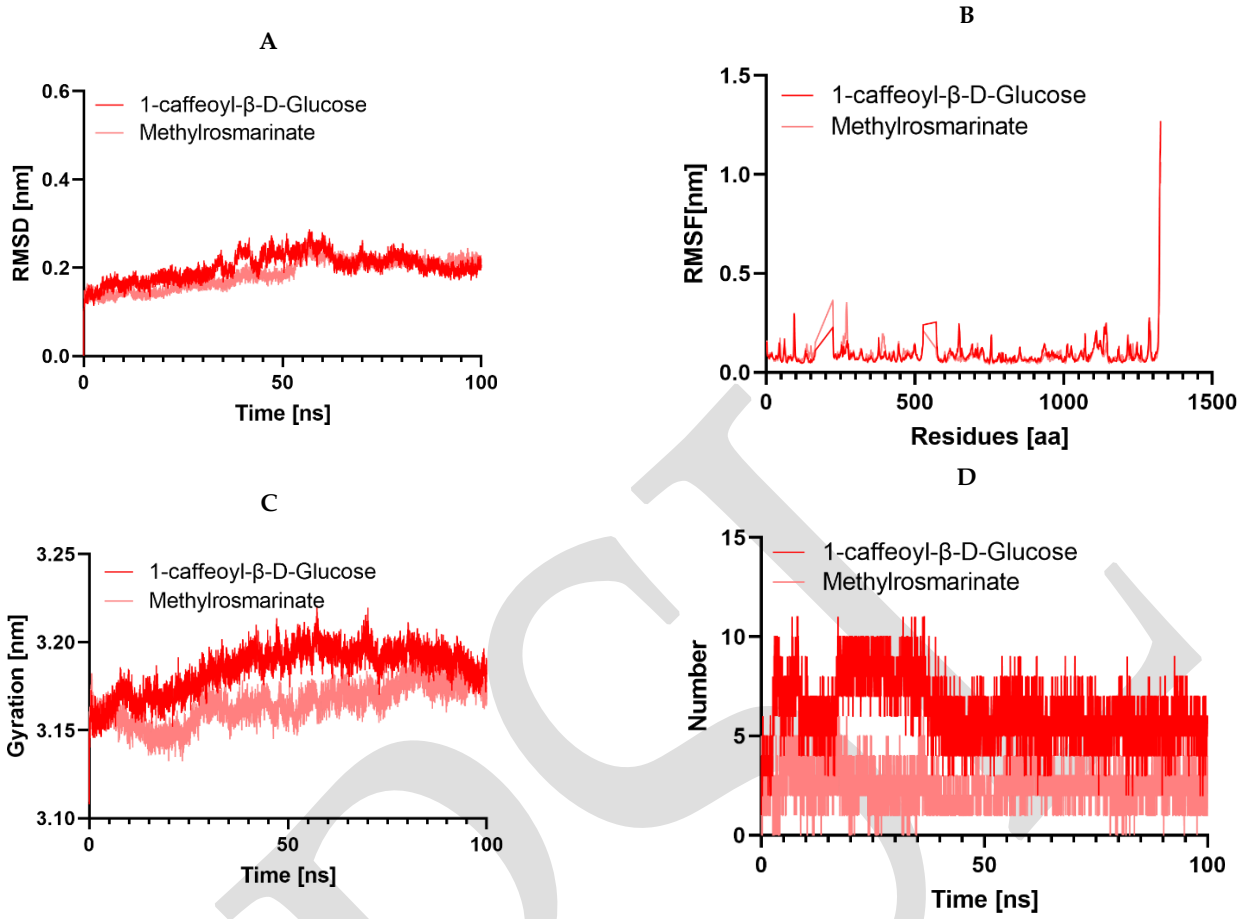

Figure 12. Structural dynamics of the 3NRZ protein: (**A**) RMSD and (**B**) RMSF. (**C**) Total number of intramolecular hydrogen bonds. (**D**) Radius of gyration.

2.11.1. Structural Dynamics of 2CAG

In this study, we delved into the structural dynamics of 2CAG through molecular dynamics simulations, focusing on their interaction with various ligands (Figure 13). Our analysis covered four different ligands (3-hydroxyflavone, Methylrosmarinate, 1-caffeoyl-β-D-Glucose, and Kaempferol), shedding light on their effects on protein conformation and dynamics. Notably, we observed strikingly similar RMSD profiles across the protein-ligand complexes, indicating minimal conformational changes upon ligand binding, except for Kaempferol, which displayed a notably higher RMSD. This suggests that while 3-hydroxyflavone, Methylrosmarinate, and 1-caffeoyl-β-D-Glucose induce negligible structural rearrangements in the protein backbone, Kaempferol triggers more pronounced changes, possibly reflecting a distinct binding mode or affinity. Further analysis of RMSF patterns revealed consistent dynamics among complexes 2CAG/3-hydroxyflavone, 2CAG/Methylrosmarinate, 2CAG/1-caffeoyl-β-D-Glucose, while the 2CAG/Kaempferol complex exhibited heightened flexibility, implying differential impacts of the ligands on protein flexibility. Examination of protein compactness using the radius of gyration (Rg) showed that 3-hydroxyflavone, Methylrosmarinate, and 1-caffeoyl-β-D-Glucose led to higher protein compactness compared to Kaempferol, correlating with the RMSD findings and suggesting tighter binding of the protein structure. Additionally, simulations unveiled the formation of hydrogen bonds between 3-hydroxyflavone, Methylrosmarinate, and 1-caffeoyl-β-D-Glucosethe target proteins over a 100 ns period, indicative of significant molecular interactions conducive to stable binding. However, Kaempferol formed fewer hydrogen bonds, implying weaker or less favorable interactions with the protein.

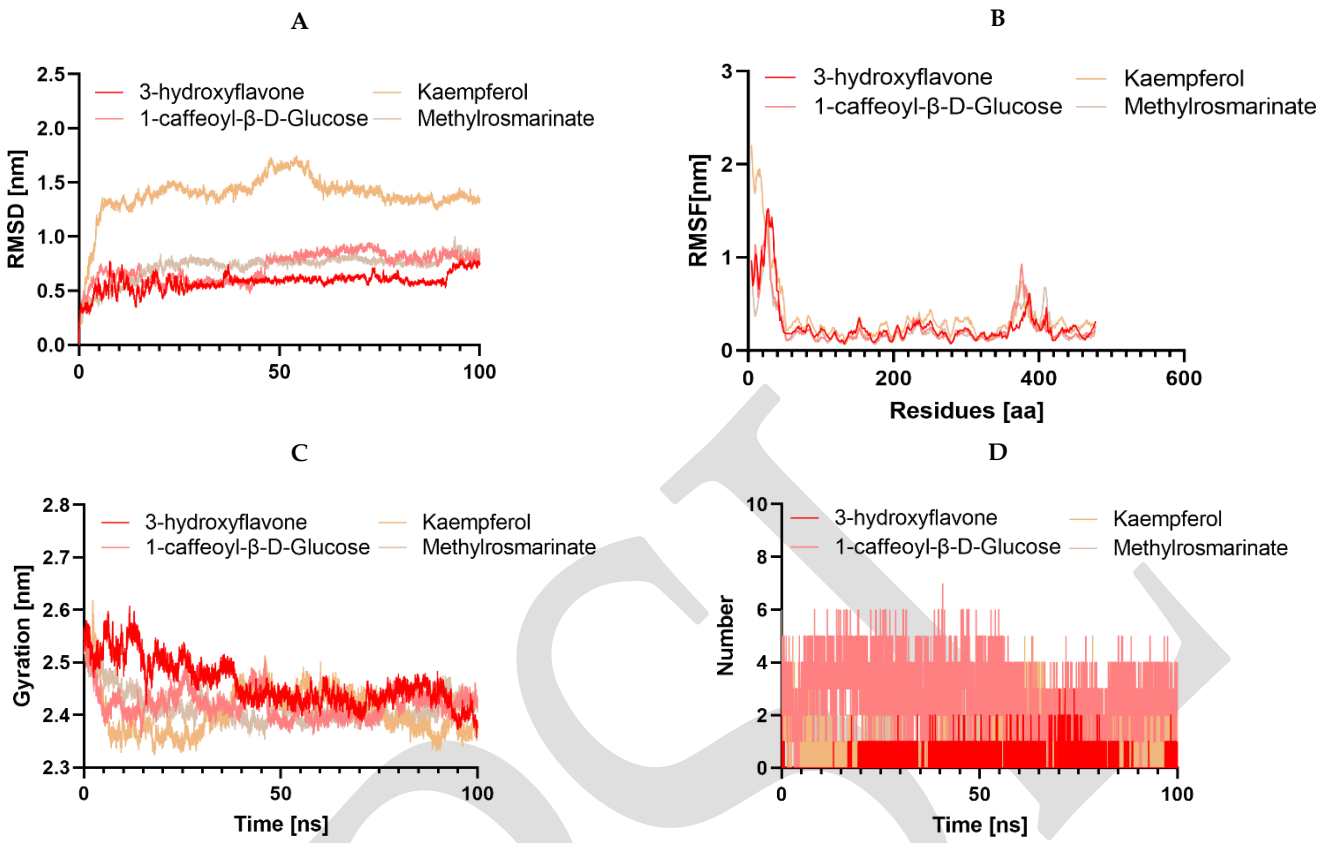

Figure 13. Structural dynamics of the 2CAG protein: (**A**) RMSD and (**B**) RMSF. (**C**) Total number of intramolecular hydrogen bonds. (**D**) Radius of gyration.

2.11.2. Structural Dynamics of 2ZDQ

3. Here, we used molecular dynamics simulations to investigate 2ZDQ's structural dynamics along with its interactions with four different ligands: emmotin H, trans-caftaric acid, methyl rosmarinate, and 1-caffeoyl-β-D-glucose. Their impact on protein dynamics and structure is illuminated by this study. The RMSD profiles of the protein-ligand complexes were quite similar, suggesting that there were only small changes in conformation when the ligands were bound, with the exception of emmotin H, which showed a much larger RMSD. Based on these results, it seems that emmotin H causes more noticeable modifications in the protein backbone than trans-caftaric acid, methyl rosmarinate, and 1-caffeoyl-β-D-glucose, which may indicate a different binding mechanism or affinity. According to further RMSF pattern analysis, the dynamics of complexes with trans-caftaric acid, methyl rosmarinate, or 1-caffeoyl-β-D-glucose were comparable. On the other hand, the emmotin H-2ZDQ complex exhibited enhanced protein flexibility, suggesting that the ligands had different impacts on this property. What followed was an examination of how these different chemicals affected the protein's structural compactness. We were able to do this by tracking the change in the radius of gyration (Rg) (Figure 14). In line with the findings of the RMSD analysis of the protein backbone, the Rg protein compactness test showed that emmotin H was outperformed by trans-caftaric acid, methyl rosmarinate, and 1-caffeoyl-β-D-Glucose. Additionally, it was shown in the simulations that trans-caftaric acid, methyl rosmarinate, or 1-caffeoyl-β-D-glucose formed hydrogen bonds with the target protein for a period of 100 ns, suggesting that there were significant molecular interactions that encouraged long-term binding. Emmotin H may have had less effective or weaker interactions with the protein because it formed fewer hydrogen bonds.

A B

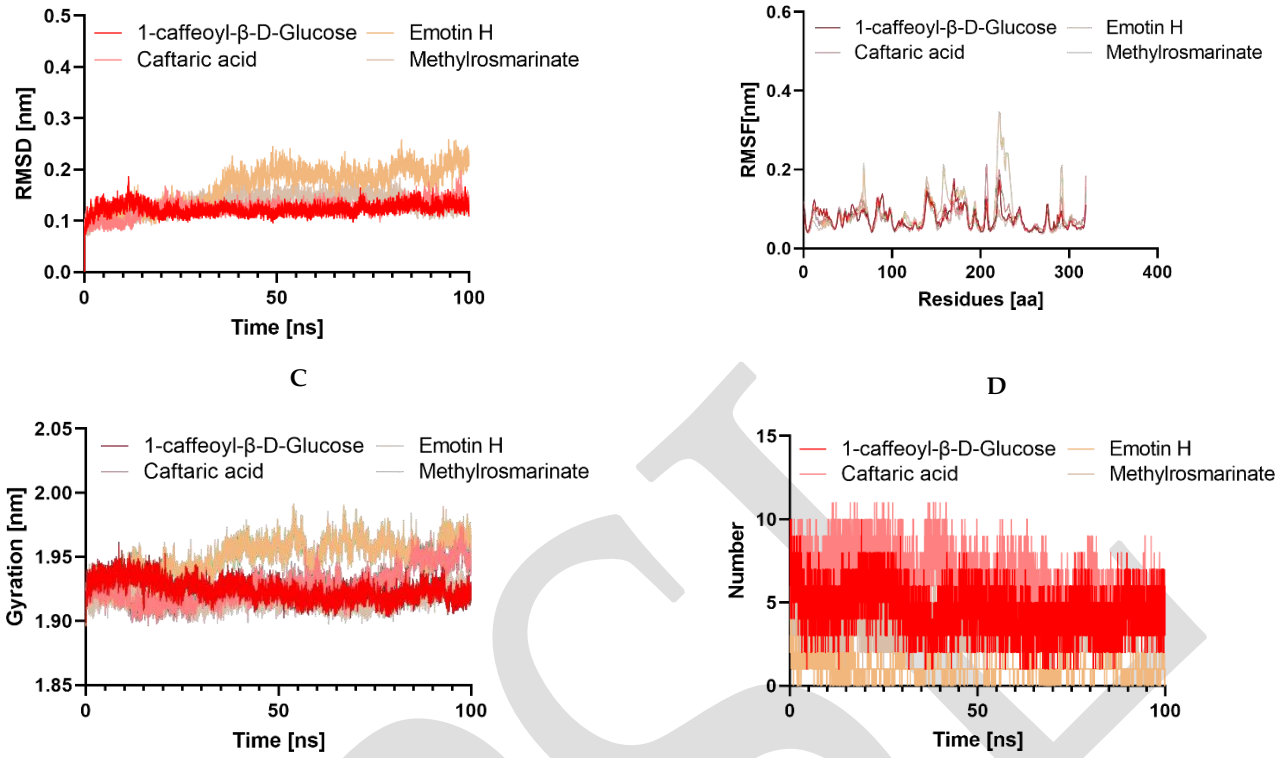

Figure 14. Structural dynamics of the 2ZDQ protein: (**A**) RMSD and (**B**) RMSF. (**C**) Total number of intramolecular hydrogen bonds. (**D**) Radius of gyration.

To design therapeutic agents and support the efficacy of the chemical composition of *A. graveolens* as a nutraceutical preservative, it is essential to analyze in detail the physicochemical characteristics of potential compounds, as well as the pharmacokinetic and physicochemical properties of the substances identified in the essential oil (EO) and aqueous extract (E_0) of *A. graveolens* seeds, comparing them to drugs. The predictive PASS and ADMET evaluations of the main constituents of the EO and aqueous extract (AE) of *A. graveolens* revealed significant values for various activities, such as antioxidant, antifungal, and antibacterial properties.

Previous research, particularly that of Najaran et al. [59], Noumi et al. [23], as well as the work of Madhuri [60], confirm the antioxidant and antimicrobial capabilities of the compounds contained in *A. graveolens*, thus suggesting their potential as therapeutic agents for various ailments. These findings highlight the exceptional qualities of the compounds identified in the EO and aqueous extract (E_0) of *A. graveolens*, which exhibit notable antioxidant, antifungal, and antibacterial activities.

The main phenolic, flavonoid, and terpenoid compounds extracted from *A. graveolens* seeds offer a wide range of pharmacological and biological applications. These compounds demonstrate promising antimicrobial, antioxidant, and anticancer properties in preclinical studies. These molecules, such as methyl rosmarinate, trans-caftaric acid, 1-caffeoyl-beta-D-glucose, kaempferol, and 3-hydroxyflavone, are currently being investigated for their biological activity. Methyl rosmarinate stands out for its antioxidative properties and antifungal activities.

It exhibits inhibitory activities against tyrosinase, α-glucosidase, and matrix metalloproteinase-1 (MMP-1) [61–64]. Trans-caffeic acid shows promise in antioxidant, anti-inflammatory, antimutagenic, anticarcinogenic, hepatoprotective, antidiabetic, antihypertensive, anti-obesity, and metabolic syndrome, as well as neuroprotective effects [65]. 1-Caffeoyl-beta-D-glucose, kaempferol, and 3-hydroxyflavone display a variety of pharmacological activities, suggesting a significant role in several therapeutic areas [66,67].

The results of our molecular docking reveal significant interactions between several bioactive compounds and various target proteins involved in antimicrobial and antioxidant activities. Among these compounds, 3-hydroxyflavone, emmotin H, trans-caftaric acid, methyl rosmarinate, 1-caffeoyl-beta-D-glucose, and kaempferol exhibited the highest binding energies with the explored proteins. These compounds have demonstrated a strong affinity with specific proteins, such as 2CAG, 2ZDQ, and 3NRZ, indicating their potential as antimicrobial and antioxidant agents. Furthermore, the study of molecular interactions using 3-hydroxyflavone revealed hydrogen bonds, Pi–alkyl bonds, Pi–cation interactions, and Pi–Pi-shaped interactions with specific catalase residues. Similarly, emmotin H formed hydrogen bonds, Pi–Pi stacking, and Pi–alkyl interactions with D-Alanine ligase residues, while trans-caftaric acid formed hydrogen bonds and Pi–Pi stacking with the latter's residues.

These specific interactions highlight the diversity of the action modes of the bioactive compounds on the target proteins. Furthermore, the analysis of catalytic residues involved in interactions with Methyl rosmarinate revealed the presence of hydrogen bonds, carbon–hydrogen bonds, Pi–Pi stacked interactions, and Pi–alkyl interactions. Additionally, interactions of this molecule with D-Alanine ligase were characterized by hydrogen bonds, carbon–hydrogen bonds, Pi–cation interactions, Pi–anion interactions, and Pi–Pi stacked interactions. Finally, interactions with 3NRZ showed hydrogen bonds, carbon-hydrogen bonds, Pi–Pi-stacked interactions, Pi–Pi-shaped interactions, and Pi–alkyl interactions. Regarding 1-Caffeoyl-beta-D-glucose, its interactions with catalase, D-Alanine ligase, and bovine xanthine oxidase were associated with different bonds, such as hydrogen bonds, carbon–hydrogen bonds, Pi–sigma interactions, Pi–Pi stacked interactions, and Pi–alkyl interactions.

Furthermore, the analysis of structural dynamics using molecular dynamics simulations provided insights into conformational changes and the stability of protein–ligand complexes [68]. These simulations revealed similar dynamic behaviors among certain complexes, as well as significant differences, suggesting distinct interaction modes and variable effects on protein flexibility and stability.

These results underscore the diversity of molecular interactions between bioactive compounds and target proteins, thus paving the way for future research in the fields of pharmaceutical chemistry and natural products.

Ultimately, despite their promising therapeutic potential, these compounds still require FDA approval for medical use, highlighting the need for further research, particularly clinical trials, to assess their efficacy and safety in patients in combating oxidative stress. These molecules are being explored for their antioxidant potential and could act as scavengers of free radicals, thereby protecting cells against oxidative stress-induced damage by modulating the expression of specific cytokines and enzymes such as SOD, dehydratase, CAT, GST, GSH, GPx, and GRd.

The antioxidant activity of *A. graveolens* essential oil, as determined by the DPPH technique and quantified by an IC_{50} value of 9.02 mg/mL, might potentially be elucidated by the findings of molecular docking investigations. Hence, compounds like trans-anethole and fenchone, which have exhibited substantial interactions with specific proteins associated with antioxidant processes, such as superoxide dismutases or catalases, may be accountable for the reported antiradical activity in laboratory settings. These compounds have electrical and structural features that are advantageous for neutralizing free radicals. This is mainly due to their phenolic or terpenic groups, which may efficiently remove reactive oxygen species.

The antifungal and antibacterial activities of the extracts and essential oils were observed to have minimum inhibitory concentrations (MICs) and minimum bactericidal concentrations (MBCs) ranging from 0.78 to 50 mg/mL and 3.125 to 6.25 µL/mL, respectively. These activities can be attributed to binding energies and interactions, such as hydrogen bonding and Van der Waals forces, which were identified in molecular docking studies. The strong attraction between emmotin H, a phenolic compound found in the

hydro-ethanolic extract, and the proteins 2ZDQ and 2CAG, which are crucial enzymes in fungi and bacteria, may account for the potent antimicrobial effects of this extract against *Aspergillus niger* and *Candida albicans*. The binding energies between emmotin H and these proteins are -10 and -9.4 kcal/mol, respectively. Undoubtedly, this type of selective molecular interaction is likely to disturb the overall structure and functional stability of these specific proteins, resulting in the suppression of the metabolic processes and development of microorganisms.

4. Materials and Methods

4.1. Plant Material

Anethum graveolens belongs to the *Apiaceae* family, commonly known as dill. The sample under study was collected from a cultivated population in the Errachidia area. Table 13 provides information on the collection location, the component harvested, and the origin. This species was identified at the Laboratory of Botany and Plant Ecology of the Scientific Institute of Rabat, Department of Botany.

Table 13. Harvesting Site, Parts Used, Habitat, and Harvesting Season for *A. graveolens*.

Scientific Name	Part Collected	Harvesting Area					
		Region	Location	Latitude (x)	Longitude (y)	Altitude (m)	Harvest Period
Anethum graveolens	Seeds	Errachidia	Annif	31°06′54″ N	5°09′38″ W	905	June 2022

4.2. Microbiological Materials

In this study, the antimicrobial activity of the essential oil (EO) and extracts of *A. graveolens* seeds was evaluated against five bacterial and five fungal strains. These microorganisms are pathogens commonly encountered in various human diseases (Table 14). These strains were isolated from the hospital environment of the Mohamed V Provincial Hospital, Meknes. All strains were stored in a 20% glycerol stock at −80 °C, rejuvenated in Mueller–Hinton and Sabouraud broths, and subcultured before use.

Table 14. List of tested bacterial and fungal strains used for antimicrobial tests.

	Strains		Abbreviations
Bacteria	Gram-negative bacilli	*Enterobacter cloacae*	*E. cloacae*
		Klebsiella pneumoniae	*K. pneumoniae*
		Escherichia coli	*E. coli*
	Gram-positive cocci	*Staphylococcus aureus*	*S. aureus*
		Staphylococcus epidermidis	*S. epidermidis*
Fungi	Yeasts	*Candida albicans*	*C. albicans*
		Candida dubliniensis	*C. dubliniensis*
		Candida tropicalis	*C. tropicalis*
		Candida parapsilosis	*C. parapsilosis*
	Mold	*Aspergillus niger*	*A. niger*

4.3. Quality Control of Plant Material

4.3.1. Moisture Content

The approach used to determine the moisture content complied with the AFNOR standard (NF-V03-402 1985) [69]. A total of 5 g of plant samples were measured using predried and pre-weighed crucibles. The crucibles, which held the plant material, were thereafter placed in an oven and exposed to a temperature ranging from 103 to 105 °C for a duration of 24 h. Subsequently, the samples were subjected to cooling in a desiccator and

subsequently weighed. The moisture content was calculated using the formula (1). The experiment was repeated three times.

$$\mathbf{MC}\% = \left(\frac{\mathbf{m_0 - m_1}}{\mathbf{m_0}}\right) \times \mathbf{100} \quad (1)$$

With m_0 as the initial mass of the plant in (g) and m_1 as the mass after drying in (g). The result is expressed as a percentage of dry matter.

4.3.2. Ash Content

The ash content refers to the amount of mineral materials that remain after the organic matter was destroyed by high-temperature incineration in a furnace. A total of 5 g of ground samples were put in a muffle furnace at a temperature of 550 °C until all charred particles were destroyed and whitish ashes were obtained, which had a consistent weight (according to NF ISO 5984) [70]. The organic matter content was determined by employing the subsequent formula (2):

$$\mathbf{OM}\% = \left(\frac{\mathbf{m_1 - m_2}}{\mathbf{TE}}\right) \times \mathbf{100} \quad (2)$$

OM%: Organic Matter
m_1: Weight of the capsule and sample before calcination
m_2: Weight of the capsule and sample after calcination
TE: Test portion
The ash content was calculated as follows (formula 3):

$$\mathbf{Ash\ \% = 100 - OM\%} \quad (3)$$

4.3.3. Heavy Metal Analysis: Inductively Coupled Plasma Atomic Emission Spectrometry (ICP-AES)

The analysis of the heavy metals in *A. graveolens* seeds was conducted using the technique of Inductively Coupled Plasma Atomic Emission Spectrometry according to the standardized mineralization protocol [71].

This method involved first preparing the sample for analysis in liquid form by mixing 0.1 g of plant powder with 3ml of aqua regia prepared from 1 mL of nitric acid HNO_3 (99%) and 2 mL of hydrochloric acid HCl (37%), all placed in a reflux setup at 200 °C for two hours to ensure the complete dissolution of residual metal particles. Following the process of chilling and decantation, the liquid remaining above the sediment was gathered. It was then passed through a filter with a pore size of 0.45 µm and brought to a volume of 15 mL by adding distilled water. The concentrations of the heavy metals including arsenic (As), cadmium (Cd), chromium (Cr), iron (Fe), lead (Pb), antimony (Sb), and titanium (Ti) were quantified using an Inductively Coupled Plasma Atomic Emission Spectrometer (Ultima 2 Jobin Yvon) at the laboratory of UATRS (Technical Support Unit for Scientific Research) at CNRST in Rabat.

4.4. Phytochemical Screening

This is a qualitative analysis that allows for the identification of primary and secondary metabolites present in *A. graveolens* seeds. These tests were based on the visual observation of color changes, and formation of precipitates and complexes, while other tests included the examination of the samples under UV light. The detection of chemical compound groups was carried out according to protocols described in previous studies [72–77].

4.5. Extraction and Quality Control of Essential Oils

4.5.1. Extraction and Determination of Essential Oil Yields

The extraction of essential oils from *A. graveolens* seeds was carried out by hydrodistillation. A total of 100 g of dried dill seeds were immersed in a 2 L flask containing 1 L of water, topped with a Clevenger apparatus and a ball-type condenser. The mixture was brought to a boil for 3 h. The oils obtained were subsequently dehydrated using anhydrous sodium sulfate (Na_2SO_4) and kept in a sealed brown glass container at a temperature of 4 °C until they were ready for use. The extraction yield of the essential oil was quantified as the volume of essential oil obtained per unit mass of plant material (v/m), using formula (4) [78].

$$\% \text{ Yield} = \left[\frac{V}{m_0 - (m_0 \times \% \text{ MC})} \times 10^4\right] \mp \text{Standard Deviation} \quad (4)$$

MC (%): Percentage of moisture in the plant material (moisture content).
m_0: Mass of distilled plant material
V: Volume of collected essential oil (in mL).

4.5.2. Analysis and Identification of the Chemical Composition of Essential Oils

5. Methods for essential oil chromatographic analysis included using a Thermo Electron gas chromatograph (Trace GC Ultra) in conjunction with a Thermo Electron Trace MS mass spectrometer (Thermo Electron: Trace GC Ultra; Polaris Q MS), with electron impact fragmentation carried out at an intensity of 70 eV. A flame ionization detector (FID) driven by an H2/Air gas mixture and a DB-5 type column (30 m × 0.25 mm × 0.25 μm film thickness) are components of the chromatograph. The column contains 5% phenyl-methyl-siloxane. During the course of 5 minutes, the temperature of the column was set to rise from 50 to 200 °C at a rate of 4 °C per minute. Using nitrogen as the carrier gas, the injection mode was divided with a leak ratio of 1/70 and a flow rate of 1 mL/min.

By comparing the essential oils' computed Kovats indices (IK) with Adams' and known reference products' IKs, we were able to determine their chemical makeup [79–81]. To do this, we compared the retention indices and mass spectra to mass spectra stored in the NIST libraries. The experimental retention indices were also compared to those in the NIST online data collection, which may be accessed at https://webbook.nist.gov/chemistry/name-ser/. in the year 2024, as of 10 April. The percentage composition reflects the automatically calculated proportions of each component based on the total ion count measured by the GC-MS.

Section 4.6: Phenolic Compound Extraction

Decoction and solid-liquid extraction using the Soxhlet device were the first steps in isolating the phenolic chemicals. To make the decoction, we first combined 30 grams of the sample with 600 milliliters of distilled water. Then, we heated the mixture to 80 degrees Celsius and let it boil for an hour. The mixture was filtered under decreased pressure after a five-minute decantation, and the decocted extract was recovered. After being dried in an oven set at 70 °C, the extract was placed in a glass vial for further use.

Two further samples, each weighing 30 g, were subjected to the solid-liquid extraction using the Soxhlet equipment. A combination of clean water and an ethanol/water ratio of 70/30 were used as extraction solvents. A rotary evaporator was used to concentrate the extracts after many cycles of extraction. Then, as shown in Table 15, these extracts were identified.

Table 15. Coding of *A. graveolens* extracts.

Extraction Methods	Solvents	Coding
Decoction	Water	E (0)
Soxhlet	Ethanol/water (70/30; *v*/*v*)	E (1)
	Water	E (2)

5.1. Quantification of Phenolic Compounds

Following Singleton and Rossi's [82] Folin-Ciocalteu technique, we calculated the total phenolic content of the various extracts. Various A. graveolens extracts include phenolic compounds with oxidizable groups; this approach relies on their reduction in a basic solution containing a combination of phosphotungstic acid H3P(W3O10)4 and phosphomolybdic acid H3PMO12O4. Using colorimetry and optical density measurement, the blue-tinted chemical compounds tungsten oxide (W8O23) and molybdenum oxide (Mo8O3) were investigated. A UV mini-1240 spectrophotometer set at 760 nm was used to measure absorbance, and it was compared to a control sample—a reaction mixture devoid of the extract—to establish statistical significance. A parallel calibration curve was also made under the same circumstances, but this time the concentration of gallic acid was set as a positive control and ranged from 0.05 to 50 μg/mL. Milligrams of gallic acid equivalent per gram of extract (mg GAE/g) was the unit of measurement for the total phenolic content, which was calculated using the calibration curve equation (Y = 0.095X + 0.003; R2 = 0.998). There were three separate runs of the experiment.

5.2. Flavonoid Quantification
We determined the flavonoid content of our samples by following the approach developed by Djeridane and colleagues, which included the use of aluminum trichloride as a reagent [83]. The process relies on this reagent oxidizing flavonoids, which creates a stable flavonoid-aluminum complex that can be seen in the visible light spectrum at 433 nm. The complex is yellowish in color. The amount of flavonoids in our samples was found by using a linear regression equation with Y = 0.073X − 0.081 and a determination coefficient R2 of 0.995, which was developed with quercetin concentrations ranging from 5 to 30 μg/mL. The amount of flavonoids was stated as milligrams of quercetin equivalent per gram of extract (mg EQ/g). The tests were conducted three times each.

5.3.1 Condensed Tannin Quantification
To measure the concentrations of condensed tannins, the vanillin technique was used [84]. Here, 20 μL of either the extracts or a solution of (+)-catechin at a concentration of 2 mg/mL was mixed with a solution of vanillin dissolved in methanol at a concentration of 4% w/v. Afterwards, the mixtures were gestated by hand. A 1.5 milliliter tube of hydrochloric acid was then used to hold each concentration. We let the reaction mixture sit at room temperature for 20 minutes. Using a blank sample as a reference, the absorbance was measured at 499 nm using a UV-visible spectrophotometer. With the catechin calibration curve (Y = 0.7421X + 0.0318; R2 = 0.998) serving as a standard, the concentration of condensed tannins in the samples was determined. There were milligrams of catechin equivalent (mg EC/g) of tannin content for each gram of extract.

5.4. Analysis of A. graveolens Seed Extracts by HPLC/UV ESI-MS
Molecular ionization techniques, including high-performance liquid chromatography (HPLC) coupled with ultraviolet light and electrospray ionization (UV-ESI-MS), were used to examine the phenolic components of A. graveolens in the decoction. An autosampler kept at 5 °C was used to conduct the analysis on an UltiMate 3000 HPLC system (Thermo Fisher Scientific, Sunnyvale, CA, USA). This HPLC setup

used a C18 reverse-phase column (Lichro CART, 250 × 4 mm, ID 5 µm, manufactured by Lichrospher, Merck, Darmstadt, Germany) at a column temperature of 40 °C. The mobile phase was made up of two solvents: solvent A and solvent B. Solvent A was a water/acetonitrile combination containing 0.1% formic acid, and solvent B was the same proportions. By using sonication, the gasses were extracted from the mobile phase. See Supplementary Table S1 for a breakdown of the components that make up the gradient. Twenty microliters (µL) was administered at a flow rate of one milliliter per minute. Broadband collision-induced dissociation (bbCID) detection was performed utilizing a Maxis Impact HD equipment (Bruker Daltonik, Bremen, Germany) after negative electrospray ionization. A diode array detector L-2455 (Merck-Hitachi, Darmstadt, Germany) was used for UV detection in the 190–600 nm range as well as the acquisition of three wavelengths ranging from 280–320–360 nm. The following values were utilized: 3000 V for the capillary voltage, 200 °C for the drying gas, 8 L/min for the dry gas flow rate, 2 bars for the nebulizer gas pressure, and 500 V for the offset voltage. The nebulizer and desolvation gas were both composed of nitrogen. From 100 to 1500, the MS data covered a wide m/z range.
Data was collected and analyzed using the Chromeleon 7.2 chromatography data system (CDS) from Thermo Scientific. By examining the mass spectra of the separated molecules, the eluted compounds were examined.

5.2. Antioxidant Activity

5.2.1. Radical Scavenging Activity by DPPH• Test

The antioxidant activity of the essential oils (EO) and extracts of *A. graveolens* was assessed using the 2,2-diphenyl-1-picrylhydrazyl (DPPH) radical, following the procedure outlined by [85]. A total of 200 µL of *A. graveolens* extract or EO was applied to test tubes containing 100% ethanol. Afterward, 2.8 mL of a solution of DPPH• in ethanol (24 µg/mL, *w/v*) was added to the mixture and allowed to incubate for 30 min in the absence of light. The measurement of absorbance was conducted at a wavelength of 515 nm using a UV–Vis spectrophotometer. The experiments were replicated thrice. The reference standard utilized was butylated hydroxytoluene (BHT) at varying concentrations. The results were quantified as a percentage of DPPH• decrease, denoted as AA% (formula 5):

$$\mathbf{AA\%} = \frac{\mathbf{A_{control}} - \mathbf{A_{Sample}}}{\mathbf{A_{control}}} \times \mathbf{100} \quad (5)$$

AA%: Percentage of antioxidant activity.
A_control: Absorbance of the solution containing only the DPPH• radical solution.
A_sample: Absorbance of the test sample solution in the presence of DPPH•.
The 50% inhibitory concentration of the DPPH• free radicals (IC_{50}) for BHT or our extracts was determined from a graph of antioxidant activity variation with concentration.

5.2.2. Ferric Reducing Antioxidant Power (FRAP) Method

The capacity of the phenolic extracts from *A. graveolens* to convert ferric iron (Fe^{3+}) in the potassium ferricyanide complex to ferrous iron (Fe^{2+}) was assessed using the technique outlined by Oyaizu [86]. The experiment consisted of combining 1 mL of the plant extract being investigated with 2.5 mL of a phosphate buffer solution (0.2 M, pH 6.6) and 2.5 mL of a potassium ferricyanide solution ($K_3Fe(CN)_6$ at a concentration of 1%). The resultant mixture was subjected to incubation in a water bath maintained at a temperature of 50 °C for a duration of 20 min. Next, 2.5 mL of a solution containing 10% trichloroacetic acid was introduced to halt the progress of the reaction. The solution was subjected to centrifugation at a speed of 3000 revolutions per minute for a duration of 10 min. Ultimately, 2.5 mL of the liquid remaining after centrifugation from each concentration was combined with 2.5 mL of pure water and 0.5 mL of a solution containing 0.1% $FeCl_3$ dissolved in

water. The absorbance of the reaction medium was measured at a wavelength of 700 nm using a UV–Vis spectrophotometer. A blank sample was generated in the same way, but

distilled water was used instead of the aqueous extract for calibration reasons. The positive control was represented by a solution of a standard antioxidant, BHA (Butylated Hydroxyanisole), for which the absorbance was measured under the same conditions as the samples. All tests were repeated three times. The graph of the variation in reducing power as a function of BHT concentration or our extracts allowed the determination of the concentration corresponding to an absorbance of 0.5 (EC_{50}).

5.2.3. Total Antioxidant Capacity

In order to determine whether the phenolic extracts of A. graveolens could transform ferric iron (Fe3+) in the potassium ferricyanide complex into ferrous iron (Fe2+), the method described by Oyaizu [86] was followed. A 1 mL sample of the plant extract under study was mixed with 2.5 mL each of a phosphate buffer solution (0.2 M, pH 6.6) and a 2.5 mL sample of potassium ferricyanide solution (K3Fe(CN)6 at a concentration of 1%) for the investigation. Twenty minutes of incubation at 50 °C was applied to the resulting mixture in a water bath. The reaction was then stopped by adding 2.5 mL of a 10% trichloroacetic acid solution. A centrifuge was used to spin the mixture at 3000 rpm for 10 minutes. Mixed with 2.5 mL of clean water and 0.5 mL of a solution containing 0.1% FeCl3 dissolved in water, 2.5 mL of the liquid left after centrifugation from each concentration was used in the end. A UV-Vis spectrophotometer was used to measure the absorbance of the reaction medium at a wavelength of 700 nm. The same procedure was used to create a blank sample, however

For the sake of accuracy in measurement, distilled water was substituted for the aqueous extract. Under the same circumstances as the samples, the absorbance of a standard antioxidant solution (BHA, butylated hydroxyanisole) served as the positive control. We ran each test three times. By plotting the changing reduction power against the concentration of BHT or our extracts, we were able to find the concentration that corresponds to an absorbance of 0.5 (EC50).

5.2.3. Oxygen Depletion Rate

To evaluate the overall antioxidant capability of A. graveolens extracts, the phosphomolybdenum assay was used, as described by Khiya et al. [87]. At acidic pH, a green complex called phosphate/Mo5+ (V) is formed, with a maximum absorbance at 695 nm. This test is based on the reduction of molybdenum Mo6+ (VI) to molybdenum Mo5+ (V) in the presence of extracts. Mixing 3 mL of the extract with 4 mM of ammonium molybdate and 28 mM of sodium phosphate made up the reactive solution. This was then put to a liter of test tube. The tubes were agitated and incubated at 95 °C for 90 minutes before being brought to room temperature. Solute absorbance at 695 nm was measured after cooling. A standard was ascorbic acid. Milligrams of ascorbic acid equivalents per gram of extract (mg AAE/g) was the unit of expression for the findings.

5.3. Activity against Microbes

A microbe's development may be entirely halted at the Minimum Inhibitory Concentration (MIC) of an essential oil or extract. Using the microdilution technique, the MIC was determined [88]. At first, the essential oil was diluted many times from a 10% DMSO stock solution until it reached concentrations ranging from 5 to 0.93 × 10−2 mg/mL. The appropriate concentrations, indicated in µg/mL, for the extracts were achieved by first preparing a stock solution and then diluting it. A final volume of 100 µL was used for each concentration when diluting the essential oil and extracts in either a Mueller-Hinton broth for bacteria or a Sabouraud broth for fungi.

The different concentrations of the dilution series were then supplemented with 100 µL of the microbial inoculum, which had a final concentration of 106 CFU/mL for bacteria and 104 CFU/mL for fungus. After incubating at 37 °C for 24 hours, 10 µL of resazurin was added to every well to detect bacterial proliferation. A change from violet to pink was seen after a further 2 hours of incubation at 37 °C, indicating the existence of microbial growth. The smallest quantity of an inhibitory agent that successfully prevents resazurin's color change is called the minimum inhibitory concentration (MIC). The growth control was located in the eleventh well of each series, while the sterility control was in the twelfth. For the oil and extracts, this procedure was repeated twice.

In each well where no apparent growth was seen, 10 µL was removed and put onto either Mueller-Hinton agar (MH) for bacteria or Sabouraud agar for fungi in order to ascertain the Minimum Bactericidal Concentration (MBC) or Minimum Fungi-cidal Concentration (MFC). The plates were left to incubate at 37 °C for eight hours. When compared to the control, the MBC and MFC samples had a 99.99% decrease in CFU/mL since they were the samples with the lowest concentrations. To measure the effectiveness against microbes, the MBC/MIC or MFC/MIC ratio was computed. When the ratio was less than 4, it meant that the essential oil had a bactericidal or

fungicidal impact; when it was larger than 4, it meant that the sample had a bacteriostatic or fungistatic effect.

5.4. PASS, ADMET, Pro-Tox, and Anticipation of the Activity of Maybe Active Substances Derived from A. graveolens Seeds Essential Oil and Water Extract

Adsorption, distribution, metabolism, excretion, and toxicity (ADMET) and PASS prediction tests were used to determine the primary components of the essential oil (EO) and water extract from A. graveolens seeds that were studied. Chemical compounds were represented using ChemBioDraw (PerkinElmer Informatics, Waltham, MA, USA, v13.0) [56]. Then, for ADMET prediction, we used the web-based programs SwissADME and pkCSM [58], in addition to the PASS- Way2Drug online prediction tool [57]. The abbreviation PASS was used to represent the possible activity (Pa) and likely inactivity (Pi) of "drug-like" compounds [89].

Toxicological characteristics such as LD50 and the toxicity class were examined, and pertinent data was gathered, using ProTox II, a practical tool developed for this purpose [90]. To evaluate the selected ligands, the ADMET software—which includes SwissADME, pkCSM, and ProTox II—was used. Their pharmacokinetics, drug-likeness, physicochemical qualities, lipophilicity, water solubility, medicinal chemistry, and toxicological aspects might all be predicted in this way. The analytical tools and procedures used in this study allowed for credible findings on the potential medicinal applications and side effects associated with the main chemical components in the essential oil and water extract of A. graveolens seeds.

5.5. Docking between molecules

The three-dimensional structures of the protein targets were obtained from the Protein Data Bank RCSB, which may be accessed at the following URL: https://www.rcsb.org/. These structures are shown in Table 16. in the year 2024, as of 10 April. Protein structures were visualized with the help of UCSF Chimera. We used Autodock Tools (version 1.5.6, The Scripps Research Institute, La Jolla, CA, USA) to build the protein structures as good docking targets. Excess water molecules, heteroatoms (hetatm), undesired protein chains, and co-crystallized ligands were removed from the protein structures during the preparation processes that preceded analysis. Then, after adding Gesteiger charges and polar hydrogen atoms, the structures were transformed to pdbqt format so they could be analyzed further.

Table 16. Protein targets and molecular docking parameters.

Protein	PDB ID	Grid Box Center Coordinates	Grid Box Size
Isoleucyl-tRNA synthetase	1JZQ	center_x = −27.803	size_x = 34
		center_y = 6.619	size_y = 22
		center_z = −28.722	size_z = 21
DNA gyrase	1KZN	center_x = 18.325	size_x = 23
		center_y = 30.783	size_y = 38
		center_z = 36.762	size_z = 38
Catalase compound II	2CAG	center_x = 60.017	size_x = 28
		center_y = 14.760	size_y = 22
		center_z = 15.935	size_z = 34
Dihydropteroate synthase	2VEG	center_x = 31.404	size_x = 24
		center_y = 48.530	size_y = 24
		center_z = 0.204	size_z = 23
D-Alanine ligase	2ZDQ	center_x = 47.378	size_x = 21
		center_y = 12.782	size_y = 26
		center_z = 5.730	size_z = 32
Dihydrofolate reductase	3SRW	center_x = -4.701	size_x = 20
		center_y = -31.536	size_y = 26

		center_z = 6.341	size_z = 26
Penicillin-binding protein 1a PBP1a	3UDI	center_x = 34.198	size_x = 24
		center_y = −1.249	size_y = 22
		center_z = 12.715	size_z = 28
Crystal structure of Staph ParE 24 kDa	4URN	center_x = -31.684	size_x = 28
		center_y = 8.021	size_y = 40
		center_z = −4.598	size_z = 42
NADPH oxidase	2CDU	center_x = 18.26	size_x = 22
		center_y = −6.35	size_y = 24
		center_z = −1.53	size_z = 28
Cytochrome P450 2C9	1OG5	center_x = −20.236	size_x = 21
		center_y = 86.761	size_y = 23
		center_z = 38.657	size_z = 20
Xanthine dehydrogenase/oxidase	3NRZ	center_x = 37.526	size_x = 20
		center_y = 19.929	size_y = 20
		center_z = 17.643	size_z = 20

The structural energy reduction process was used to the sixteen compounds' three-dimensional models based on their individual structures, which were retrieved from PubChem. After that, the ligands' SDF files were transformed into pdbqt formats using the Prescription Virtual Screening Python script (AutoDock Vina 1.2.0). An AutoDock Vina scoring function was used in the compound docking procedure. The Vina control included placing a grid box on top of the protein structure after choosing the ligand and protein molecules to dock with. Prior to starting the docking process using the AutoDock Vina application, the grid box size might be modified according to the selected active site residues. Table 16 shows that the size and location of the grid box were determined by coordinates in such a way that they perfectly encircled the active binding site, thereby limiting the search area. We used PyMOL to analyze the ligand-protein binding characteristics and collected the resultant data for docked molecules as free binding energy values.

The next step was to use redocking, which is a dependable technique for validating the molecular docking procedure. The crystallized ligand is first removed from the protein using this technique, and then a fresh docking study is conducted in the same region as the first one. By thoroughly examining the RMSD parameter value using specialist tools like PyMOL 2.5.0, we may correctly determine whether the docked ligand overlaps with the crystalline ligand using this technique. In conclusion, redocking provides independent verification of the accuracy of molecular docking studies.

5.3 Macromolecular Modeling

To assess the protein-ligand complex's stability, molecular dynamics simulations were conducted using the GROMACS 2019.3 program [91]. The CGenFF service was used to build the ligand topologies, and the protein was analyzed using the all-atom CHARMM36 force field. By adding ions to balance the total charges, the systems were declared neutral when all complexes were immersed in a rectangular container filled with TIP3P water molecules. In order to minimize energy consumption while maximizing force, a force threshold (Fmax) of 1000 kJ/mol/nm was chosen using the steepest descent approach. Molecular dynamics simulation research kept the ensembles at constant NVT (number of atoms, volume and temperature) and NPT (number of atoms, pressure and temperature). The next step was to run 100 ns molecular dynamics simulations on each molecule. We gained a thorough grasp of protein behavior by analyzing output trajectories.

Section 5.4: Analyzing Statistics

The results are shown as an average, and the standard deviation is used to indicate how

variable they are. A one-way ANOVA test and Tukey's post-test were used to examine the data in GraphPad Prism 8 (version 8.0.2, San Diego, CA, USA). Values of P less than 0.05 were considered statistically significant. We used the Pearson correlation coefficient to look for a link between the phenolic chemicals and the amount of antioxidant activity. When the p-value was less than 0.05, we said that the difference was statistically significant.

6. Conclusions

The high concentration of phytochemicals in Anethum graveolens seeds was the main focus of this investigation. The GC-MS analysis of the essential oil revealed that, with an abundance of 38.13%, (E)-anethole was the most abundant chemical, followed by 29.32% for estragole, 17.21% for fenchone, and 7.37% for α-pinene. Additionally, the seeds included secondary metabolites such as mucilage, triterpenes, tannins, flavonoids, and sterols.
The results of this quantitative analysis showed that there were high levels of polyphenols, flavonoids, and concentrated tannins. Umbelliferone(12.35%), hydroxyflavone(11.23%), rosmanol(8.95%), biotin (8.36%), Emmotin H(4.91%), and cuma-rin (4.21%) were among the 38 notable chemicals detected and identified by HPLC/UV-ESI-MS analytical methods.

The DPPH$_{\cdot}$, FRAP, and CAT assays demonstrated that the essential oils and extracts had a strong antioxidant effect. Both metal ion binding and free radical neutralization were successfully accomplished by them. In terms of effectiveness against most of the bacteria examined, the antimicrobial tests showed that the essential oil was superior to the aqueous, ethanolic, and decoction extracts. Because its main ingredients work together synergistically, it is more effective than before.
Molecular dynamics and docking simulations confirmed strong interactions and long-term stability between many bioactive compounds and several target proteins.
According to the results, A. graveolens has great potential as a natural food preservative and a treatment for a variety of human ailments.

Supplementary Materials: The following supporting information can be downloaded at https://www.mdpi.com/article/10.3390/ph17070862/s1, Figure S1. GC-MS chromatogram of the essential oil from A. graveolens; Figure S2. Structures of the main compounds identified in A. graveolens EO; Figure S3. HPLC chromatogram of compounds from the decocted extract of A. graveolens; Figure S4. Structures of the majority of compounds identified in extract E (0) of A. graveolens; Table S1. Gradient mobile phase elution.

Author Contributions: Conceptualization, N.H. and A.D.; methodology, N.H. and A.A.S.; software, M.R.; validation, T.Z. and A.B.; formal analysis, S.B.; investigation, N.H. and F.R.; resources, T.Z.; data curation, E.M.B.; writing—original draft preparation, N.H. and A.D.; writing—review and editing, N.H., A.A.S. and A.D.; visualization, I.T.; supervision, A.B.; project administration, T.Z.; funding acquisition, A.A.S. All authors have read and agreed to the published version of the manuscript.

Funding: This research was funded by Researchers supporting project number (RSPD2024R1057), King Saud University, Riyadh, Saudi Arabia.

Institutional Review Board Statement: Not applicable.

Informed Consent Statement: Not applicable.

Data Availability Statement: Data are contained within this article.

Acknowledgments: Authors are thankful to the Researchers supporting project number (RSPD2024R1057), King Saud University, Riyadh, Saudi Arabia.

Conflicts of Interest: The authors declare that they have no known competing financial interests or personal relationships that could have appeared to influence the work reported in this paper.

References

1. Mathers, C.; Organization, W.H. *The Global Burden of Disease: 2004 Update*; World Health Organization: Geneva, Switzerland, 2008; ISBN 978-92-4-156371-0.
2. Zhang, X.-J.; Diao, M.; Zhang, Y.-F. A Review of the Occurrence, Metabolites and Health Risks of Butylated Hydroxyanisole (BHA). *J. Sci. Food Agric.* **2023**, *103*, 6150–6166. https://doi.org/10.1002/jsfa.12676.
3. Ito, N.; Hirose, M.; Fukushima, S.; Tsuda, H.; Shirai, T.; Tatematsu, M. Studies on Antioxidants: Their Carcinogenic and Modifying Effects on Chemical Carcinogenesis. *Food Chem. Toxicol.* **1986**, *24*, 1071–1082. https://doi.org/10.1016/0278-6915(86)90291-7.
4. Lopez-Romero, J.C.; González-Ríos, H.; Borges, A.; Simões, M. Antibacterial Effects and Mode of Action of Selected Essential Oils Components against Escherichia Coli and Staphylococcus Aureus. *Evid. Based Complement. Altern. Med.* **2015**, *2015*. https://doi.org/10.1155/2015/795435.
5. Paven, C.S.J.; Radu, D.; Alexa, E.; Pintilie, S.; Rivis, A. *Anethum Graveolens*—An Important Source of Antioxidant Compounds for Food Industry. *Adv. Biotechnol.* **2018**, *18*, 11–18. https://doi.org/10.5593/sgem2018/6.2/S25.002.
6. Jana, S.; Shekhawat, G. Anethum Graveolens: An Indian Traditional Medicinal Herb and Spice. *Pharmacogn. Rev.* **2010**, *4*, 179–184. https://doi.org/10.4103/0973-7847.70915.
7. Brinsi, C.; Selmi, H.; Jedidi, S.; Sebai, H. Enquête Ethno-Pharmacologique Sur l' Usage Traditionnel de l'Aneth (Anethum Graveolens L.) Dans Le Nord-Ouest de La Tunisie. *Rev. Marocaine Des Sci. Agron. Et Vétérinaires* **2022**, *10*, 282–286.
8. Jirovetz, L.; Buchbauer, G.; Stoyanova, A.S.; Georgiev, E.V.; Damianova, S.T.; Composition, Quality Control, and Antimicrobial Activity of the Essential Oil of Long-Time Stored Dill (*Anethum Graveolens*, L.) Seeds from Bulgaria. *J. Agric. Food Chem.* **2003**, *51*, 3854–3857. https://doi.org/10.1021/jf030004y.
9. Kaur, N.; Chahal, K.K.; Kumar, A.; Singh, R.; Bhardwaj, U. Antioxidant Activity of *Anethum Graveolens*, L. Essential Oil Constituents and Their Chemical Analogues. *J. Food Biochem.* **2019**, *43*, e12782. https://doi.org/10.1111/jfbc.12782.
10. Nam, H.H.; Nan, L.; Choo, B.K. Anti-Inflammation and Protective Effects of Anethum Graveolens l. (Dill Seeds) on Esophageal Mucosa Damages in Reflux Esophagitis-Induced Rats. *Foods* **2021**, *10*. https://doi.org/10.3390/foods10102500.
11. Goodarzi, M.T.; Khodadadi, I.; Tavilani, H.; Abbasi Oshaghi, E. The Role of Anethum Graveolens, L. (Dill) in the Management of Diabetes. *J. Trop. Med.* **2016**, *2016*. https://doi.org/10.1155/2016/1098916.
12. Ozliman, S.; Yaldiz, G.; Camlica, M.; Ozsoy, N. Chemical Components of Essential Oils and Biological Activities of the Aqueous Extract of Anethum Graveolens, L. Grown under Inorganic and Organic Conditions. *Chem. Biol. Technol. Agric.* **2021**, *8*, 1–16. https://doi.org/10.1186/s40538-021-00224-9.
13. Mahran, G.H.; Kadry, H.A.; Isaac, Z.G.; Thabet, C.K.; Al-Azizi, M.M.; El-Olemy, M.M. Investigation of Diuretic Drug Plants. 1. Phytochemical Screening and Pharmacological Evaluation of Anethum Graveolens, L., Apium Graveolens, L., Daucus Carota, L. and Eruca Sativa Mill. *Phytother. Res.* **1991**, *5*, 169–172. https://doi.org/10.1002/ptr.2650050406.
14. Najafzadeh, R.; Ghasemzadeh, S.; Mirfakhraie, S. Effect of Essential Oils from Nepeta Crispa, Anethum Graveolens and Satureja Hortensis Against the Stored-Product Insect "Ephestia Kuehniella (Zeller)." *J. Med. Plants By-Prod.* **2019**, *2*, 163–169.
15. Rabeh, N.M.; Aboraya, A.O. Hepatoprotective Effect of Dill (Anethum Graveolens, L.) and Fennel (Foeniculum Vulgare) Oil on Hepatotoxic Rats. *Pak. J. Nutr.* **2014**, *13*, 303–309. https://doi.org/10.3923/pjn.2014.303.309.
16. Al-Oqail, M.M.; Farshori, N.N. Antioxidant and Anticancer Efficacies of Anethum Graveolens against Human Breast Carcinoma Cells through Oxidative Stress and Caspase Dependency. *BioMed Res. Int.* **2021**, *2021*. https://doi.org/10.1155/2021/5535570.
17. El-Sayed, K.K.; El-Sheikh, E.-S.A.; Sherif, R.M.; Gouhar, K.A. Chemical Composition and Bio-Efficacy of Essential Oils Isolated from Seeds of Anethum Graveolens, L., Leaves of Thymus Vulgaris, L., and Nuts of Myristica Fragrans Houtt. Against Callosobruchus Maculatus (Fab.) (Coleoptera: Bruchidae). *J. Essent. Oil Bear. Plants* **2021**, *24*, 1402–1414. https://doi.org/10.1080/0972060X.2021.2016498.
18. Farmanpour Kalalagh, K.; Mohebodini, M.; Fattahi, R.; Beyraghdar Kashkooli, A.; Davarpanah Dizaj, S.; Salehifar, F.; Mokhtari, A.M. Drying Temperatures Affect the Qualitative–Quantitative Variation of Aromatic Profiling in Anethum Graveolens, L. Ecotypes as an Industrial–Medicinal–Vegetable Plant. *Front. Plant Sci.* **2023**, *14*. https://doi.org/10.3389/fpls.2023.1137840.
19. Mehdizadeh, T.; Mojaddar Langroodi, A.; Shakouri, R.; Khorshidi, S.; Physicochemical, Microbiological, and Sensory Characteristics of Probiotic Yogurt Enhanced with Anethum Graveolens Essential Oil. *J. Food Saf.* **2019**, *39*, e12683. https://doi.org/10.1111/jfs.12683.
20. Znini, M.; Ansari, A.; Costa, J.; Senhaji, O.; Paolini, J.; Majidi, L.; Experimental, Quantum Chemical and Molecular Dynamic Simulations Studies on the Corrosion Inhibition of C38 Steel in 1M HCl by Anethum Graveolens Essential Oil. *Anal. Bioanal. Electrochem* **2019**, *11*, 1426–1451.
21. Li, H.; Zhou, W.; Hu, Y.; Mo, H.; Wang, J.; Hu, L. GC-MS Analysis of Essential Oil from Anethum Graveolens L (Dill) Seeds Extracted by Supercritical Carbon Dioxide. *Trop. J. Pharm. Res.* **2019**, *18*, 1291–1296. https://doi.org/10.4314/tjpr.v18i6.21.
22. Snuossi, M.; Trabelsi, N.; Ben Taleb, S.; Dehmeni, A.; Flamini, G.; De Feo, V. Laurus Nobilis, Zingiber Officinale and Anethum Graveolens Essential Oils: Composition, Antioxidant and Antibacterial Activities against Bacteria Isolated from Fish and Shellfish. *Molecules* **2016**, *21*, 1414. https://doi.org/10.3390/molecules21101414.
23. Noumi, E.; Ahmad, I.; Adnan, M.; Merghni, A.; Patel, H.; Haddaji, N.; Bouali, N.; Alabbosh, K.F.; Ghannay, S.; Aouadi, K.; et al. GC/MS Profiling, Antibacterial, Anti-Quorum Sensing, and Antibiofilm Properties of Anethum Graveolens, L. Essential Oil: Molecular Docking Study and In-Silico ADME Profiling. *Plants* **2023**, *12*, 1997. https://doi.org/10.3390/plants12101997.
24. Kostić, I.; Lazarević, J.; Šešlija Jovanović, D.; Kostić, M.; Marković, T.; Milanović, S. Potential of Essential Oils from Anise, Dill and Fennel Seeds for the Gypsy Moth Control. *Plants* **2021**, *10*, 2194. https://doi.org/10.3390/plants10102194.

25. Aati, H.Y.; Perveen, S.; Aati, S.; Orfali, R.; Alqahtani, J.H.; Al-Taweel, A.M.; Wanner, J.; Aati, A.Y. Headspace Solid-Phase Microextraction Method for Extracting Volatile Constituents from the Different Parts of Saudi Anethum Graveolens, L. and Their Antimicrobial Activity. *Heliyon* **2022**, *8*. https://doi.org/10.1016/j.heliyon.2022.e09051.
26. Anvar, N.; Nateghi, L.; Shariatifar, N.; Mousavi, S.A. The Effect of Essential Oil of Anethum Graveolens, L. Seed and Gallic Acid (Free and Nano Forms) on Microbial, Chemical and Sensory Characteristics in Minced Meat during Storage at 4 °C. *Food Chem. X* **2023**, *19*, 100842. https://doi.org/10.1016/j.fochx.2023.100842.
27. El Mansouri, L.; Bousta, D.; Balouiri, M.; Ouedrhiri, W.; Elyoubi-El Hamsas, A. Antioxidant Activity of Aqueous Seed Extract of Anethum Graveolens, L. *Int. J. Pharm. Sci. Res.* **2016**, *7*, 1219–1223. https://doi.org/10.13040/IJPSR.0975-8232.7(3).1219-23.
28. Bota, S.R.; Stanasel, O.D.; Blidar, C.F.; Serban, G. Phenolic Constituents of Anethum Graveolens Seed Extracts: Chemical Profile and Antioxidant Effect Studies. *J. Pharm. Res. Int.* **2021**, *33*, 168–179. https://doi.org/10.9734/jpri/2021/v33i54b33777.
29. Mashraqi, A. Induction Role of Chitosan Nanoparticles to Anethum Graveolens Extract against Food-Borne Bacteria, Oxidant, and Diabetic Activities in Vitro. *Front. Microbiol.* **2023**, *14*, 1–12. https://doi.org/10.3389/fmicb.2023.1209524.
30. Erdogan Orhan, I.; Senol, F.S.; Ozturk, N.; Celik, S.A.; Pulur, A.; Kan, Y. Phytochemical Contents and Enzyme Inhibitory and Antioxidant Properties of Anethum Graveolens, L. (Dill) Samples Cultivated under Organic and Conventional Agricultural Conditions. *Food Chem. Toxicol.* **2013**, *59*, 96–103. https://doi.org/10.1016/j.fct.2013.05.053.
31. Meena, S.S.; Lal, G.; Dubey, P.N.; Meena, M.D.; Ravi, Y. Medicinal and Therapeutic Uses of Dill (Anethum Graveolens L.)—A Review. *Int. J. Seed Spices* **2019**, *9*, 14–20.
32. Sharifi-Rad, J.; Cruz-Martins, N.; López-Jornet, P.; Lopez, E.P.F.; Harun, N.; Yeskaliyeva, B.; Beyatli, A.; Sytar, O.; Shaheen, S.; Sharopov, F.; et al. Natural Coumarins: Exploring the Pharmacological Complexity and Underlying Molecular Mechanisms. *Oxidative Med. Cell. Longev.* **2021**, *2021*. https://doi.org/10.1155/2021/6492346.
33. Mazimba, O. Umbelliferone: Sources, Chemistry and Bioactivities Review. *Bull. Fac. Pharm. Cairo Univ.* **2017**, *55*, 223–232. https://doi.org/10.1016/j.bfopcu.2017.05.001.
34. Chen, S.; Wang, X.; Cheng, Y.; Gao, H.; Chen, X. A Review of Classification, Biosynthesis, Biological Activities and Potential Applications of Flavonoids. *Molecules* **2023**, *28*, 1–27. https://doi.org/10.3390/molecules28134982.
35. Thomas, S.D.; Jha, N.K.; Jha, S.K.; Sadek, B.; Ojha, S. Pharmacological and Molecular Insight on the Cardioprotective Role of Apigenin. *Nutrients* **2023**, *15*. https://doi.org/10.3390/nu15020385.
36. Abid, R.; Ghazanfar, S.; Farid, A.; Sulaman, S.M.; Idrees, M.; Amen, R.A.; Muzammal, M.; Shahzad, M.K.; Mohamed, M.O.; Khaled, A.A.; et al. Pharmacological Properties of 4′, 5, 7-Trihydroxyflavone (Apigenin) and Its Impact on Cell Signaling Pathways. *Molecules* **2022**, *27*, 1–20. https://doi.org/10.3390/molecules27134304.
37. Maneesai, P.; Potue, P.; Khamseekaew, J.; Sangartit, W.; Rattanakanokchai, S.; Poasakate, A.; Pakdeechote, P. Kaempferol Protects against Cardiovascular Abnormalities Induced by Nitric Oxide Deficiency in Rats by Suppressing the TNF-α Pathway. *Eur. J. Pharmacol.* **2023**, *960*, 176112. https://doi.org/10.1016/j.ejphar.2023.176112.
38. Deng, H.; Xu, Q.; Guo, H.Y.; Huang, X.; Chen, F.; Jin, L.; Quan, Z.S.; Shen, Q.K. Application of Cinnamic Acid in the Structural Modification of Natural Products: A Review. *Phytochemistry* **2023**, *206*, 113532.
39. Ruwizhi, N.; Aderibigbe, B.A. Cinnamic Acid Derivatives and Their Biological Efficacy. *Int. J. Mol. Sci.* **2020**, *21*, 1–36. https://doi.org/10.3390/ijms21165712.
40. Babaeenezhad, E.; Nouryazdan, N.; Nasri, M.; Ahmadvand, H.; Moradi Sarabi, M. Cinnamic Acid Ameliorate Gentamicin-Induced Liver Dysfunctions and Nephrotoxicity in Rats through Induction of Antioxidant Activities. *Heliyon* **2021**, *7*, e07465. https://doi.org/10.1016/j.heliyon.2021.e07465.
41. Koczurkiewicz-Adamczyk, P.; Klaś, K.; Gunia-Krzyżak, A.; Piska, K.; Andrysiak, K.; Stępniewski, J.; Lasota, S.; Wójcik-Pszczoła, K.; Dulak, J.; Madeja, Z.; et al. Cinnamic Acid Derivatives as Cardioprotective Agents against Oxidative and Structural Damage Induced by Doxorubicin. *Int. J. Mol. Sci.* **2021**, *22*. https://doi.org/10.3390/ijms22126217.
42. Osanloo, M.; Ghanbariasad, A.; Taghinezhad, A. Antioxidant and Anticancer Activities of Anethum Graveolens, L., Citrus Limon (L.) Osbeck and Zingiber Officinale Roscoe Essential Oils. *Tradit. Integr. Med.* **2021**, 333–347. https://doi.org/10.18502/tim.v6i4.8266.
43. Gladikostić, N.; Ikonić, B.; Teslić, N.; Zeković, Z.; Božović, D.; Putnik, P.; Bursać Kovačević, D.; Pavlić, B. Essential Oils from Apiaceae, Asteraceae, Cupressaceae and Lamiaceae Families Grown in Serbia: Comparative Chemical Profiling with In Vitro Antioxidant Activity. *Plants* **2023**, *12*, 745. https://doi.org/10.3390/plants12040745.
44. Stanojević, L.P.; Radulović, N.S.; Djokić, T.M.; Stanković, B.M.; Ilić, D.P.; Cakić, M.D.; Nikolić, V.D. The Yield, Composition and Hydrodistillation Kinetics of the Essential Oil of Dill Seeds (*Anethi Fructus*) Obtained by Different Hydrodistillation Techniques. *Ind. Crops Prod.* **2015**, *65*, 429–436. https://doi.org/10.1016/j.indcrop.2014.10.067.
45. Galicka, A.; Krętowski, R.; Nazaruk, J.; Cechowska-Pasko, M. Anethole Prevents Hydrogen Peroxide-Induced Apoptosis and Collagen Metabolism Alterations in Human Skin Fibroblasts. *Mol Cell Biochem* **2014**, *394*, 217–224. https://doi.org/10.1007/s11010-014-2097-0.
46. Donati, M.; Mondin, A.; Chen, Z.; Miranda, F.M.; do Nascimento Jr, B.B.; Schirato, G.; Pastore, P.; Froldi, G. Radical Scavenging and Antimicrobial Activities of Croton Zehntneri, Pterodon Emarginatus and Schinopsis Brasiliensis Essential Oils and Their Major Constituents: Estragole, Trans-Anethole, β-Caryophyllene and Myrcene. *Nat. Prod. Res.* **2015**, *29*, 939–946. https://doi.org/10.1080/14786419.2014.964709.

47. Senatore, F.; Oliviero, F.; Scandolera, E.; Taglialatela-Scafati, O.; Roscigno, G.; Zaccardelli, M.; De Falco, E. Chemical Composition, Antimicrobial and Antioxidant Activities of Anethole-Rich Oil from Leaves of Selected Varieties of Fennel [*Foeniculum Vulgare* Mill. Ssp. *Vulgare* Var. *Azoricum* (Mill.) Thell]. *Fitoterapia* **2013**, *90*, 214–219. https://doi.org/10.1016/j.fitote.2013.07.021.
48. Luís, Â.; Sousa, S.; Wackerlig, J.; Dobusch, D.; Duarte, A.P.; Pereira, L.; Domingues, F. Star Anise (*Illicium Verum* Hook. f.) Essential Oil: Antioxidant Properties and Antibacterial Activity against *Acinetobacter Baumannii*. *Flavour Fragr. J.* **2019**, *34*, 260–270. https://doi.org/10.1002/ffj.3498.
49. Singh, S.; Das, S.; Singh, G.; Perotti, M.; Schuff, C.; Catalan, C. Comparative Studies of Chemical Composition, Antioxidant and Antimicrobial Potentials of Essential Oils and Oleoresins Obtained from Seeds and Leaves of Anethum Graveolens, L. *Toxicol. Open Access* **2017**, *3*, 2–9.
50. Coêlho, M.L.; Islam, M.T.; Laylson da Silva Oliveira, G.; Oliveira Barros de Alencar, M.V.; Victor de Oliveira Santos, J.; Campinho dos Reis, A.; Oliveira Ferreira da Mata, A.M.; Correia Jardim Paz, M.F.; Docea, A.O.; Calina, D.; et al. Cytotoxic and Antioxidant Properties of Natural Bioactive Monoterpenes Nerol, Estragole, and 3,7-Dimethyl-1-Octanol. *Adv. Pharmacol. Pharm. Sci.* **2022**, *2022*, e8002766. https://doi.org/10.1155/2022/8002766.
51. El Omari, N.; Balahbib, A.; Bakrim, S.; Benali, T.; Ullah, R.; Alotaibi, A.; Naceiri El Mrabti, H.; Goh, B.H.; Ong, S.-K.; Ming, L.C.; et al. Fenchone and Camphor: Main Natural Compounds from Lavandula Stoechas, L., Expediting Multiple in Vitro Biological Activities. *Heliyon* **2023**, *9*, e21222. https://doi.org/10.1016/j.heliyon.2023.e21222.
52. Singh, A.; Raja, W. Assessment of Antioxidant Activity of Foeniculum Vulgare Seed Extract Using Fenton Reaction. *Res. J. Med. Plants Ayurveda* **2020**, *1*, 1–7.
53. Basavegowda, J.; Raveesha, K.A.R.; Amruthesh, K.N. Bioactivity and Phytochemical Studies of Seed Extracts of Anethum Graveolens Linn. *Lett. Appl. NanoBioScience* **2022**, *11*, 3560–3572. https://doi.org/10.33263/LIANBS112.35603572.
54. Kaur, G.J.; Arora, D.S. Antibacterial and Phytochemical Screening of Anethum Graveolens, Foeniculum Vulgare and Trachyspermum Ammi. *BMC Complement. Altern. Med.* **2009**, *9*, 1–10. https://doi.org/10.1186/1472-6882-9-30.
55. Mota, A.S.; Rosário Martins, M.; Arantes, S.; Lopes, V.R.; Bettencourt, E.; Pombal, S.; Gomes, A.C.; Silva, L.A. Antimicrobial Activity and Chemical Composition of the Essential Oils of Portuguese Foeniculum Vulgare Fruits. *Nat. Prod. Commun.* **2015**, *10*, 673–676. https://doi.org/10.1177/1934578x1501000437.
56. Li, Z.; Wan, H.; Shi, Y.; Ouyang, P. Personal Experience with Four Kinds of Chemical Structure Drawing Software: Review on ChemDraw, ChemWindow, ISIS/Draw, and ChemSketch. *J. Chem. Inf. Comput. Sci.* **2004**, *44*, 1886–1890. https://doi.org/10.1021/ci049794h.
57. Filimonov, D.A.; Lagunin, A.A.; Gloriozova, T.A.; Rudik, A.V.; Druzhilovskii, D.S.; Pogodin, P.V.; Poroikov, V.V. Prediction of the Biological Activity Spectra of Organic Compounds Using the Pass Online Web Resource. *Chem Heterocycl Comp* **2014**, *50*, 444–457. https://doi.org/10.1007/s10593-014-1496-1.
58. Daina, A.; Michielin, O.; Zoete, V. SwissADME: A Free Web Tool to Evaluate Pharmacokinetics, Drug-Likeness and Medicinal Chemistry Friendliness of Small Molecules. *Sci. Rep.* **2017**, *7*, 42717.
59. Najaran, Z.T.; Hassanzadeh, M.K.; Nasery, M.; Emami, S.A. Dill (*Anethum Graveolens*, L.) Oils. In *Essential Oils in Food Preservation, Flavor and Safety*; Preedy, V.R., Ed.; Academic Press: San Diego, CA, USA, 2016; pp. 405–412. ISBN 978-0-12-416641-7.
60. Madhuri, J.V. Bioactivity of *Anethum Graveolens*–An in Silico Approach. *New Vis. Biol. Sci.* **2022**, *13*, 85.
61. Suriyarak, S.; Bayrasy, C.; Schmidt, H.; Villeneuve, P.; Weiss, J. Impact of Fatty Acid Chain Length of Rosmarinate Esters on Their Antimicrobial Activity against Staphylococcus Carnosus LTH1502 and Escherichia Coli K-12 LTH4263. *J Food Prot* **2013**, *76*, 1539–1548. https://doi.org/10.4315/0362-028X.JFP-12-254.
62. Lin, L.; Dong, Y.; Zhao, H.; Wen, L.; Yang, B.; Zhao, M. Comparative Evaluation of Rosmarinic Acid, Methyl Rosmarinate and Pedalitin Isolated from Rabdosia Serra (MAXIM.) HARA as Inhibitors of Tyrosinase and α-Glucosidase. *Food Chem* **2011**, *129*, 884–889. https://doi.org/10.1016/j.foodchem.2011.05.039.
63. Yuan, H.; Lu, W.; Wang, L.; Shan, L.; Li, H.; Huang, J.; Sun, Q.; Zhang, W. Synthesis of Derivatives of Methyl Rosmarinate and Their Inhibitory Activities against Matrix Metalloproteinase-1 (MMP-1). *Eur J Med Chem* **2013**, *62*, 148–157. https://doi.org/10.1016/j.ejmech.2012.09.047.
64. Woo, E.-R.; Piao, M.S. Antioxidative Constituents from Lycopus Lucidus. *Arch Pharm Res* **2004**, *27*, 173–176. https://doi.org/10.1007/BF02980102.
65. Koriem, K.M.M. Caftaric Acid: An Overview on Its Structure, Daily Consumption, Bioavailability and Pharmacological Effects. *Biointerface Res. Appl. Chem* **2020**, *10*, 5616–5623.
66. Parveen, S.; Bhat, I.U.H.; Bhat, R. Kaempferol and Its Derivatives: Biological Activities and Therapeutic Potential. *Asian Pac. J. Trop. Biomed.* **2023**, *13*, 411. https://doi.org/10.4103/2221-1691.387747.
67. Tambe, V.; Ditani, A.; Rajpoot, K.; Tekade, R.K. Chapter 4—Pharmacokinetics Aspects of Structural Modifications in Drug Design and Therapy. In *Biopharmaceutics and Pharmacokinetics Considerations*; Tekade, R.K., Ed.; Advances in Pharmaceutical Product Development and Research; Academic Press: Cambridge, MA, USA, 2021; Volume 1, pp. 83–108. ISBN 978-0-12-814425-1.
68. Hirano, Y.; Okimoto, N.; Fujita, S.; Taiji, M. Molecular Dynamics Study of Conformational Changes of Tankyrase 2 Binding Subsites upon Ligand Binding. *ACS Omega* **2021**, *6*, 17609–17620. https://doi.org/10.1021/acsomega.1c02159.
69. AFNOR NF V03-402. Épices et Aromates—Détermination de la Teneur en Eau—Méthode par Entraînement. Available online: https://www.boutique.afnor.org/fr-fr/norme/nf-v03402/epices-et-aromates-determination-de-la-teneur-en-eau-methode-par-entraineme/fa032462/325 (accessed on 4 October 2021).
70. Ph. Eur. 11.0, 0125 (04/2023), 2022 Animal Feeding Stuffs—Determination of Crude Ash. ISO: Geneva, Switzerland, 2022.

71. Skujins, S. *Handbook for ICP-AES (Varian-Vista): A Short Guide to Vista Series ICP-AES Operation*; Varian Int. AG: Zug, Switzerland, 1998; p. 1.
72. Dohou, N.; Yamni, K.; Tahrouch, S.; Idrissi Hassani, L.M.; Badoc, A.; Gmira, N. Screening Phytochimique d'une Endémique Ibéro-Marocaine, Thymelaea Lythroides. *Bull. De La Société De Pharm. De Bordx.* **2003**, *142*, 61–78.
73. Mezzoug, N.; Elhadri, A.; Dallouh, A.; Amkiss, S.; Skali, N.S.; Abrini, J.; Zhiri, A.; Baudoux, D.; Diallo, B.; El Jaziri, M.; et al. Investigation of the Mutagenic and Antimutagenic Effects of Origanum Compactum Essential Oil and Some of Its Constituents. *Mutat. Res. /Genet. Toxicol. Environ. Mutagen.* **2007**, *629*, 100–110. https://doi.org/10.1016/J.MRGENTOX.2007.01.011.
74. Mogode, D.J. Etude Phytochimique et Pharmacologique de Cassia Nigricans Vahl (Caesalpiniaceae) Utilisé Dans Le Traitement Des Dermatoses Au Tchad. Thèse de Doctorat, Université de N'Djaména, Abidjan, Tchad, 2005.
75. Bruneton, J. *PHARMACOGNOSIE, PHYTOCHIMIE, PLANTES MEDICINALES (4E ED.)*; LAVOISIER: Paris, France, 2009; ISBN 2743019042.
76. Bekro, Y.-A.; Mamyrbekova Békro, J.A.; Boua, B.B.; Fézan, H.T.B.; Ehile, E.E. Étude Ethnobotanique et Screening Phytochimique de Caesalpinia Benthamiana (Baill.) Herend. et Zarucchi (Caesalpiniaceae). *Sci. Nat.* **2007**, *4*, 217–225,Abidjan.
77. N'Guessan, K.; Kadja, B.; Zirihi, G.; Traoré, D.; Aké-Assi, L. Screening phytochimique de quelques plantes médicinales ivoiriennes utilisées en pays Krobou (Agboville, Côte-d'Ivoire). *Sci. Nat.* **2009**, *6*, 1–15. https://doi.org/10.4314/scinat.v6i1.48575.
78. Akrout, A.; Chemli, R.; Chref, I.; Hammami, M. Analysis of the Essential Oil of Artemisia Campestris, L. *Flavour Fragr. J.* **2001**, *16*, 337–339. https://doi.org/10.1002/ffj.1006.
79. Adams, R.P. *Identification of Essential Oil Components by Gas Chromatography/Mass Spectrometry*; Allured publishing corporation Carol Stream, IL, USA, 2007; Vol. 456.
80. Babushok, V.I.; Linstrom, P.J.; Zenkevich, I.G. Retention Indices for Frequently Reported Compounds of Plant Essential Oils. *J. Phys. Chem. Ref. Data* **2011**, *40*, 043101. https://doi.org/10.1063/1.3653552.
81. Kovats, E.S. Gas Chromatographic Characterization of Organic Substances in the Retention Index System. *Adv. Chromatogr.* **1965**, *1*, 229–247.
82. Singleton, V.L.; Rossi, J.A. Colorimetry of Total Phenolics with Phosphomolybdic-Phosphotungstic Acid Reagents. *Am. J. Enol. Vitic.* **1965**, *16*, 144–158. https://doi.org/10.5344/AJEV.1965.16.3.144.
83. Djeridane, A.; Yousfi, M.; Nadjemi, B.; Boutassouna, D.; Stocker, P.; Vidal, N. Antioxidant Activity of Some Algerian Medicinal Plants Extracts Containing Phenolic Compounds. *Food Chem.* **2006**, *97*, 654–660. https://doi.org/10.1016/j.foodchem.2005.04.028.
84. Price, M.L.; Scoyoc, S.V.; Butler, L.G. A Critical Evaluation of the Vanillin Reaction as an Assay for Tannin in Sorghum Grain. *J. Agric. Food Chem.* **1978**, *26*, 1214–1218. https://doi.org/10.1021/JF60219A031/ASSET/JF60219A031.FP.PNG_V03.
85. Liu, M.H.; Otsuka, N.; Noyori, K.; Shiota, S.; Ogawa, W.; Kuroda, T.; Hatano, T.; Tsuchiya, T. Synergistic Effect of Kaempferol Glycosides Purified from Laurus Nobilis and Fluoroquinolones on Methicillin-Resistant Staphylococcus Aureus. *Biol. Pharm. Bull.* **2009**, *32*, 489–492. https://doi.org/10.1248/bpb.32.489.
86. Oyaizu, M. Studies on Products of Browning Reaction. Antioxidative Activities of Products of Browning Reaction Prepared from Glucosamine. *Jpn. J. Nutr. Diet.* **1986**, *44*, 307–315. https://doi.org/10.5264/EIYOGAKUZASHI.44.307.
87. Khiya, Z.; Oualcadi, Y.; Gamar, A.; Berrekhis, F.; Zair, T.; Hilali, F.E.L. Correlation of Total Polyphenolic Content with Antioxidant Activity of Hydromethanolic Extract and Their Fractions of the Salvia Officinalis Leaves from Different Regions of Morocco. *J. Chem.* **2021**, *2021*, 1–11. https://doi.org/10.1155/2021/8585313.
88. Drioiche, A.; Baammi, S.; Zibouh, K.; Al Kamaly, O.; Alnakhli, A.M.; Remok, F.; Saidi, S.; Amaiach, R.; El Makhoukhi, F.; Elomri, A. A Study of the Synergistic Effects of Essential Oils from Origanum Compactum and Origanum Elongatum with Commercial Antibiotics against Highly Prioritized Multidrug-Resistant Bacteria for the World Health Organization. *Metabolites* **2024**, *14*, 210.
89. Alam, A.; Jawaid, T.; Alam, P. In Vitro Antioxidant and Anti-Inflammatory Activities of Green Cardamom Essential Oil and in Silico Molecular Docking of Its Major Bioactives. *J. Taibah Univ. Sci.* **2021**, *15*, 757–768. https://doi.org/10.1080/16583655.2021.2002550.
90. Banerjee, P.; Eckert, A.O.; Schrey, A.K.; Preissner, R. ProTox-II: A Webserver for the Prediction of Toxicity of Chemicals. *Nucleic Acids Res.* **2018**, *46*, W257–W263. https://doi.org/10.1093/nar/gky318.
91. Van Der Spoel, D.; Lindahl, E.; Hess, B.; Groenhof, G.; Mark, A.E.; Berendsen, H.J.C. GROMACS: Fast, Flexible, and Free. *J Comput Chem* **2005**, *26*, 1701–1718. https://doi.org/10.1002/jcc.20291.